
Article:
Fonnesu, M, Patacci, M, Haughton, PDW et al. (2016) Hybrid Event Beds Generated By Local Substrate Delamination On A Confined-Basin Floor. Journal of Sedimentary Research, 86 (8). pp. 929-943. ISSN: 1527-1404

https://doi.org/10.2110/jsr.2016.58

HYBRID EVENT BEDS GENERATED BY LOCAL SUBSTRATE DELAMINATION ON A CONFINED BASIN FLOOR

MARCO FONNESU[1], MARCO PATACCI[2], PETER D.W. HAUGHTON[1], FABRIZIO FELLETTI[3] AND WILLIAM D. McCAFFREY[2]

[1]UCD School of Earth Sciences, University College Dublin, Belfield, Dublin 4, Ireland

[2]Turbidites Research Group, School of Earth and Environment, University of Leeds, Leeds LS2 9JT, UK

[3]Dipartimento di Scienze della Terra, Università degli Studi di Milano, Via Mangiagalli 34, 20034 Milano, Italy

Keywords: turbidites, hybrid event beds, substrate delamination, scours, basin plain, entrainment

ABSTRACT

The outer parts of deep-water fans, and the basin plains into which they pass, are often described as areas where erosion is negligible and turbidite systems have net aggradation. Nevertheless sedimentological and stratigraphic analysis of outer fan lobe and confined basin plain deposits in Cretaceous-Paleocene Gottero Sandstone (NW of Italy) has revealed extensive but cryptic bedding-parallel substrate-delamination features at the base of many sheet-like event beds. These comprise a variety of shallow but wide scour structures showing evidence of lateral expansion by sand-injection. The scours commonly occur at the base of beds made up of a basal clean sandstone overlain by argillaceous sandstone containing abundant mudstone clasts and locally large substrate rafts (up to 20 meters long). These strata are interpreted as a type of hybrid event bed. Field observations suggest that mud-clast entrainment occurred by delamination at the base of dense sandy flows. The large rafts, in some cases only partly detached, were incorporated in the flows locally and then carried for short distances (100s m to a few km) before partly disaggregating and undergoing deformation due to internal shearing. The development of such features may be

common in flat and/or confined basin settings where high-volume flows interact with a cohesive and well layered substrate (e.g. muddy outer fans or confined or ponded basins with thick mudstone caps). Delamination is therefore suggested as an alternative mechanism leading to the formation of hybrid event beds following local substrate entrainment on the basin floor as opposed to on more remote slopes and at channel-lobe transition zones.

INTRODUCTION

Turbidity currents can both erode and deposit as they pass from slope to basin floor. Erosion occurs mainly along proximal, higher-gradient and more constricted sectors of the flow pathway where turbidity currents accelerate, bulk up and exert high bed shear stress (Hall et al., 2008; Fildani et al., 2013). Over time, net erosion can form canyons, channel systems and scour fields that are often well imaged on the modern sea floor (Pirmez et al., 2000), in seismic time-slices of ancient systems (Mayall and Stewart, 2000; Fonnesu, 2003; Kolla et al., 2007) and in outcrop (Mutti and Normark, 1987; Brunt and McCaffrey, 2007; Hubbard et al., 2014). Erosion can also occur at gradient breaks and flow expansion points due to hydraulic jumps, so scour features are often present in channel lobe transition zones (Mutti and Normark, 1987; Mutti, 1992; Wynn et al., 2002; Van der Merwe et al., 2014; Hofstra et al., 2016) and proximal lobe settings (Etienne et al., 2012; Burgreen and Graham, 2014). Although shallow distributive channels can extend distally to the outer parts of some lobes (Johnson et al., 2001; Beaubouef et al., 2003; Hodgson et al., 2006), lobe fringes and the basin plain systems with which they interfinger are generally low relief areas dominated by depositional flows with negligible erosional capacity (Pilkey, 1987). Successions ascribed to these settings are often characterized by a tabular bedding geometry consistent with little erosion. However, this inference may be deceptive. The evaluation of erosion based simply on overall bed geometry can be misleading as the planar bases of turbidites may hide flat or stepped erosion surfaces (Eggenhuisen et al., 2011). If present, distal erosion could have important implications for the system architecture (i.e. sea floor levelling and bed compensation, vertical sandstone amalgamation) and for the

dynamics of flows on low gradient basin floors (see Eggenhuisen et al., 2010; Eggenhuisen and McCaffrey, 2012).

The study described here demonstrates significant yet cryptic erosion in outer fan lobe and confined basin plain sheet deposits of the Cretaceous-Paleocene Gottero Sandstone cropping out on Mount Ramaceto and Mount Zatta (NW Apennines, Italy). These extensive exposures permit high-resolution bed correlations that identify where substrate has been removed and incorporated into many of the thicker event beds. In addition, the M. Ramaceto succession is inverted (Casnedi, 1982) and this means that unusually extensive exposures of bed bases occur on dip slopes where the planform geometry of basal features can be documented. Both outcrops show an important association between scours features and sandstone beds with concentrations of mudstone clasts or central argillaceous and mudclast-rich sandstone divisions resembling hybrid event beds (HEBs; Haughton et al., 2009).

Most models for hybrid event bed formation stress up-dip incorporation of clays and/or mud clasts that then modify flow behavior through turbulence damping (e.g. Haughton et al., 2003; Talling et al., 2004; Baas et al., 2009; Sumner et al., 2009;; Talling, 2013). Thus although typically found down dip in outer fan and basin floor settings, their origin is often sought in the up-dip erosive sector, or even in the original slope failures (Haughton et al., 2003; Talling , 2013). Little emphasis has been placed on erosion and entrainment directly from the basin floor (but see Puigdefàbregas et al. 2004; Talling et al., 2004; Hodgson, 2009; and Muzzi Magalhaes and Tinterri, 2010). In the examples discussed here, large quantities of substrate mud were locally entrained, forcing partial flow transformations. There may thus be a class of hybrid event bed in which down-dip flow evolution is linked to local basin floor rather than up-dip substrate interactions.

The study of the Gottero outcrops described below addresses three main questions: i) how is erosion achieved in what was the outer part of the system? ii) can the erosion be linked to local

hybrid event bed development?; and iii) what factors might promote hybrid flow generation in outer fan and confined basin plain settings?

METHODS AND TERMINOLOGY

The study is based on an extensive dataset from the M. Ramaceto and M. Zatta outcrops of the Cretaceous-Paleocene Gottero system (Fig. 1A). Over 3800 m of measured logs capturing detail at cm-scale were collected in the two areas along 10 transects. These are used to frame the overall stratigraphic architecture, the geometry of individual sandbodies and to document the pattern of erosion beneath individual event beds. In addition, closely spaced (10s m apart) serial vertical logs and maps of the erosional features on exposed bed bases were acquired for specific beds. A high-precision Jacob's staff with rotatable laser pointer (Patacci, 2016) was used in conjunction with a measuring stick to collect accurate thickness measurements. Paleoflow orientations were determined using a geological compass and corrected for structural dip. Textures of selected beds have been analyzed using optical microscopy (11 thin sections). Clay content and the framework mineralogy were quantified petrographically by point counting (500 points per section).

The terminology used in this paper is as follows. We use the term event bed to describe the deposit left by the passage of a single sediment gravity flow (Kneller and McCaffrey, 2003). The term hybrid event bed refers to the deposits of a flow varying from poorly cohesive and essentially turbulent through to increasingly cohesive and turbulence-suppressed flow (Haughton et al., 2009). In an idealized deposit, this is commonly expressed by an upward transition from a basal clean sandstone via banded sandstone to argillaceous sandstone with common mudstone clasts. Many hybrid event beds also have a capping, structured sandstone-mudstone couplet emplaced by a turbulent wake. Recent studies have highlighted significant variability in hybrid event bed make-up including the texture of the argillaceous sandstone division. This is thought to reflect variable extent of turbulence damping, different modes of flow partitioning, and deposits that are frozen at different stages in the transformation process (Baas et al., 2009; 2011; Kane and Pontén, 2012; Patacci et al. 2014; Fonnesu

et al., 2015). Hybrid event beds can thus span a range of bed expressions and inferred flow processes but the common factor is evidence for flow transformation driven by incorporation or segregation of clay and/or mud clasts. This may involve turbulent fractionation of mud clasts and other grains (e.g. mica flakes and organic matter) but also includes substrate clasts entrained in the base of flows that then are carried in a shearing boundary layer. A complete spectrum is recognized from mud clasts buried by sand rapidly falling out of suspension (mudstone clast-rich turbidites), through mud clasts that are carried in traction to concentrations of mud clasts and sand that travel and arrest *en-masse* (e.g. Patacci et al. 2014). Herein mud/mudstone clast refers to equant cm to m-scale pieces of substrate entrained in the flows; raft refers to large substrate slabs with long axes much greater than the bed thickness (2-20 m); mud/mudstone chips refer to mm-scale fragments.

The study focuses on the outer parts of the Gottero system spanning both outer fan lobe and confined basin plain settings. Many deep-water settings comprise fan systems characterized by distributive channels and terminal lobes that pass down slope into lateral equivalent basin plain sheet systems (Mutti, 1977; Mutti and Johns, 1978; Mutti and Normark, 1987; Piper and Normark, 2001, Remacha et al., 2005; Mutti et al., 2009; Pickering and Hiscott, 2015). The former are dominated by lobes, tongue-shaped deposits made up of offset compensationally-stacked lobe elements (Mutti and Sonnino, 1981; Prélat et al. 2009) producing variable but commonly organized vertical bed thickness trends including but not restricted to thickening upwards cycles (Prélat and Hodgson, 2013). Although they are sheet-like over 100s of m, the lobe elements taper and compensate at longer length scales. Outer fan lobe refers to the down-dip extension of the lobes (see Mutti and Normark, 1987) where beds are thinner, finer grained and less commonly amalgamated compared to more proximal counterparts. Basin plain sheet systems are characterized by laterally-extensive sheet-like beds that extend many kilometers with minimal change in thickness and poor vertical organization at m to of 10s m scales. Although basin plains are commonly mud-prone, those developed in confined and tectonically active settings are generally sandier (Pickering and Hiscott, 2015), with thick mud (-stone) caps to sand (-stone) beds developed where flows are

ponded (Mutti and Johns, 1978; Remacha et al., 2005; Mutti et al., 2009). Fan-attached basin plain sheet systems commonly have abundant thin-beds emplaced by flows that deposited most of their load on up-current lobes, but also important coarser and thicker event beds left by exceptionally large flows that bypassed the up-slope lobe region and deposited mainly on the adjacent basin plain (Piper and Normark, 2001; Remacha et al., 2005).

GOTTERO SYSTEM GEOLOGICAL SETTING

The Gottero Sandstone crops out discontinuously along the eastern Ligurian coast and immediately inland in the Ligurian Apennines between Genova and Carrara, in north-western Italy (Fig. 1A). It represents a deep-sea fan and related basin plain sheet system (Nilsen and Abbate, 1984) of Maastrichtian to Early Paleocene age (Monechi and Treves, 1984) that developed during convergence between Europe and Adria when sand was supplied to a trench developed in front of the growing Alpine accretionary prism (Marroni et al., 2004). The sand was sourced from Hercynian granites and associated metamorphic rocks of the Corsica-Sardinia massif, with sediment transport from south to the north and northeast (Parea, 1965; Nilsen and Abbate, 1984) consistent with paleoflow data collected during the present study (Fig. 1A). The Gottero system overlies Jurassic ophiolitic crust (Bortolotti and Passerini, 1970) and a Valanginian-Santonian basinal sequence comprising the Diaspri Shale, Calpionella Limestone, Palombini Shale and Lavagna Slates that formed in the Ligurian-Piedemont Sea (Fig. 1B). It is unconformably overlain by the early Paleocene Giaiette Shales (Passerini and Pirini, 1964) which constitute a large (>300 m thick) chaotic unit (mass transport complex; MTC) interpreted as the collapse of the accretionary wedge (Marroni and Pandolfi, 2001). The Gottero Sandstone and the Ligurian sequence were subsequently extensively deformed during the Eocene and Oligocene becoming one of several allochthonous units within the *Internal Liguridi* of the Northern Apennines (Gottero Unit - Abbate and Sagri, 1970).

Proximal-to-distal facies associations and lateral grain-size trends are developed in the Gottero system (Fig. 1A; Nilsen and Abbate, 1984). The lack of continuous exposures precludes precise

correlation of individual stratigraphic elements but the Gottero Sandstone itself and the enclosing stratigraphic units can be consistently mapped across the area (Marini, 1992). The more proximal system (inner fan) is located in the SW sector of the basin and is characterized by fine-grained slope deposits and pebbly to coarse sand grade channel fills, interpreted as part of the feeder system. The intermediate area (mid-fan) crops out mostly along the Ligurian coast and is dominated by thick coarse to very coarse grained amalgamated sandstone lobes overlain by a sequence of thinner lobe packages separated by intervening mudstone deposits. The distal part of the system ('outer fan' of Nilsen and Abbate, 1984) and focus of this study, is located to the north and west and is characterized by lobe stacks and a thick succession of laterally extensive sheet-like event beds (Casnedi, 1982; Nilsen and Abbate, 1984).

Distal Gottero succession

The north-western and distal sector of the system crops out in the M. Ramaceto and M. Zatta areas (at least 50 km away from the up-dip feeder channels without taking account of tectonic shortening; Nilsen and Abbate, 1984). The two distal sections may represent separate depocenters (Marini, 1992; 1995) with a maximum thickness of 1075 m on M. Ramaceto (Fig. 1B). The two successions reveal that the Gottero system commenced with a rapid progradational or growth trend from thin-bedded basin plain and fan fringe deposits to proximal amalgamated sandstone lobes. In the M. Zatta area the succession continued with a stack of outer fan lobes characterized by thick and coarse grained sandstone beds and mudstone clast-rich hybrid event beds (32% of the beds > 30 cm thick are of hybrid character; 103 HEBs in total). In the M. Ramaceteo area, the upper Gottero succession is characterized by a monotonous stack of thick, relatively coarse grained and tabular sandy beds (i.e. sheets) with a high percentage of mudstone clast-rich hybrid event beds (58 % of the beds > 30 cm thick; 125 HEBs in total) alternating with thin fine-grained and laminated beds. Individual beds can be traced in the field for up to a kilometer normal to paleoflow and up to 4 km down-dip without significant thickness changes but with a high degree of internal facies variability in the case

of the hybrid event beds (Fig. 2; Fonnesu et al., 2015). In both areas, the non-hybrid thick event beds are composed of un-structured to weakly laminated coarse to medium grained sandstone grading into laminated and/or current rippled fine-grained sandstone to siltstone at the top. These are interpreted as deposits of high-density turbidity currents. Centimeter-size mudstone clasts are often present and typically clustered in the uppermost unstructured bed portion (see Fonnesu et al., 2015). Mudstone clast-rich facies are commonly observed in beds that can be correlated downdip or laterally to hybrid event beds and therefore are considered to be genetically related to them. Repetition of structured and unstructured sandstone, wavy sinusoidal laminations and silty caps with pseudonodules in the uppermost part of both hybrid beds and turbidites are common and interpreted to represent the effect of deflection or ponding of the dilute parts of the flow (Pickering and Hiscott, 1985; Remacha et al., 2005; Haughton et al., 2001; Patacci et al., 2015). The overall thickness of individual event beds and their associated mudstone caps tends to increase upwards in M. Ramaceto section, together with increasingly common structures indicative of flow deflection or ponding. This is interpreted to record a change to a higher degree of basin confinement (Sinclair and Tomasso, 2002) due to the on-going Alpine collision and growth of intrabasinal relief that helped to isolate parts of the trench (i.e. Bracco relief of Elter and Raggi, 1965). A change in the composition of some sandstone beds towards the top of the succession, with an increase of ophiolite-derived material (Pandolfi, 1997), is consistent with increasing down-dip confinement by a rising accretionary complex. Although the relationship between the distal outcrops and the down-dip basin margin is not preserved, the aggrading sheet-like geometry of the thick and laterally continuous event beds are consistent with a confined basin plain setting in which the deposits of the largest volume flows were trapped.

EROSIONAL AND DELAMINATION FEATURES AT BED BASES

Many of the beds comprising the distal portion of the Gottero system have extensive but often cryptic erosional bases that are revealed in inverted exposures of bed soles and by detailed km-range correlations that identify where substrate is missing beneath event beds.

Planform and 3D geometry

A number of beds in the distal Gottero succession have bases characterized by multiphase erosional features expressed at a range of scales, although their recognition is usually difficult in sections normal to bedding. It is therefore likely that the occurrence of these features is routinely overlooked. Their geometry is especially evident in plan-view on the inverted base of Bed 14 in the M. Ramaceto outcrop (Fig. 3). Bed 14 is a 2.3 m thick tripartite bed (or hybrid event bed *sensu* Haughton et al., 2009 and see earlier) made up of: i) a graded basal, very coarse to medium grade, generally unstructured and relatively clean sandstone (10% average of dispersed clay) with isolated floating mudstone clasts that are more abundant at the top of this division. Occasional sheet and dish dewatering features are observed. ii) A central chaotic mudstone clast-rich (clasts up to 25 cm in size) muddy sandstone with a dispersed clay volume of about 20% increasing towards the top; and an upper division iii) of graded fine to very fine sand to silt grade with parallel lamination developed in the sandstone. The event bed has an overall tabular geometry with minimal thickness changes when traced along the M. Ramaceto exposure for more than 3 km in the direction of the palaeoflow and about 1 km across strike. Bed 14 was deposited above a 3.20 m thick mudstone interval including abundant scattered diagenetic carbonate nodules ("Septarie level" of Andri and Zavatteri, 1990). This is overlain by a 0.05 m thick limestone bed and then by a 0.25 m thick mudstone interval. The thin limestone bed has been used as a datum in order to quantify the minimum amount of erosion that took place beneath Bed 14.

The bed base is made up of a terraced surface reflecting three levels of substrate erosion (Fig. 4A). These are developed on bedding-parallel surfaces at c. 25, 19 and 12 cm respectively above the

limestone datum. The shallowest level (Tier 1) is covered by small-scale grooves, minor flutes and rare prod marks. Sole structures are densely spaced and uniformly distributed across the entire surface and aligned along an average 295° N paleoflow orientation with a very small dispersion (Fig. 4B). The sole marks on the first surface are clearly cross-cut by deeper elongated scour features (Fig. 4C, 4D) that coalesced to excavate the sea floor in patches down to a mid-level bedding-parallel surface (Tier 2). Individual Tier 2 scours are 0.4 to 1.5 m across and 1 to 5 m long and have distinctive asymmetric edges in flow transverse cross-sections, generally with step-like and wing-like edges (Fig. 4E). Mudstone pieces in the act of being detached from the muddy substrate are often found beneath the undercut scour margins (Fig. 4F). When the elongated scour features have fallen away from the outcrop it is possible to observe the internal sandstone fill which includes a surface with a prominent lineation oriented orthogonal to the axis of elongation of the scour (Fig. 4G). The surface is present in the sand 4-5 cm above the Tier 1 surface (having rotated the bed back to its original orientation) but it plunges down into the Tier 2 scours where it is at the level of Tier 1. The main orientation of Tier 2 scour features is similar to those on Tier 1 (mean orientation 298° N based on scour edges) but with a slightly higher dispersion. Sparse grooves are present on the Tier 2 surface but are much less abundant than on the first level. The Tier 2 surface is further incised by the deepest scours (Tier 3). They are the smallest scour features (10s cm wide), filled with the coarsest sediment (very coarse sand) and are patchily distributed along the outcrop. Their orientation is similar to the other features (297° N based on their edges) but the dispersion is again slightly larger than for the Tier 1 and 2 features.

Although the full extent of the scour field cannot be determined due to the limited dimension of the outcrop, the composite erosional feature is at least 150 m wide and 40 m long. When traced down current, individual (Tier 2) scours coalesce and form a compound erosion surface in the central part of the outcrop; towards the top of the outcrop and further downstream, the scours become more isolated again (Fig. 3C), suggesting the full length of the scour feature is unlikely to be much greater than the 40 meters observed.

Erosional features inferred from detailed bed-to-bed correlations

Several 0.5 to 2 m deep and 100s m wide erosional features can be constrained at bed bases by the detailed bed-to-bed correlations along the M. Ramaceto outcrop (Fig. 5). The minimum amount of substrate erosion can be inferred where at least part of the removed stratigraphic succession is preserved in-situ laterally. It can be more confidently estimated where a thin-bedded sequence is deposited just beneath the bed (rather than a thick mudstone interval) allowing progressive removal of stratigraphy to be tracked as the erosion surface steps down through these layers. The surface between a thin-bedded package and a thick mudstone interval below often acts as the preferred surface along which deeply-eroded sectors extend flat for several hundred meters before stepping up again. Sites where the erosion process is arrested in progress are only rarely observed. A revealing example is seen at the base of an outer fan lobe from the lower part of the M. Zatta succession (Fig. 6). This shows the lateral juxtaposition of a sandy event bed and a 1.1 m thick interval of laminated mudstones and thin beds in a section mostly at a high angle to paleoflow direction. A coarse-grained sandstone sill a few centimeters thick extends from the base of the sandstone bed along the boundary between the thin-bedded package and the homogenous mudstone cap to an earlier event bed.

The event beds that were deposited above some of the deepest substrate erosion features are typically very thick (2.5 m to 6 m thick) tripartite hybrid event beds with a chaotic and mud-rich central division sandwiched between lower structureless or weakly graded, clean coarse-grained sandstone and upper normally graded fine-grained sandstone to siltstone with parallel lamination and/or a rippled top. The chaotic divisions can have a variety of complex textures but in many cases are dominated by large rafts (up to 20 m across in some cases, but commonly of meter scale) surrounded by injected coarse-grained sandstone coming from the basal sandy division or by a mudstone clast-rich sand-mud mixture (typically containing ~18-20% dispersed clay). The rafts may be composed exclusively of mudstone, or they may comprise pieces of thin-bedded stratigraphy,

sometimes still in a bedding-parallel orientation but in other cases intensely folded or partly distended in pinch-and-swell structures (Fig. 7). The presence of intact or deformed thin-bedded rafts is typical of event beds that have a similar *in-situ* thin-bedded section beneath them somewhere along the bed correlation (Fig. 5; Fig. 7B-C). Where hybrid event beds directly overlie a thick mudstone interval without thin beds, the rafts are only made of mudstone (Fig. 7A). When the larger rafts are present they often plough into the basal sand and extensively modify the previously just deposited sand (Fonnesu et al., 2015). The area of raft accumulation often corresponds spatially to the sector with the deepest substrate erosion beneath the bed (Beds 8, 15.4 and 17.3 of Fig. 5).

INTERPRETATION OF EROSIONAL AND DEPOSITIONAL FEATURES

The various erosive features (10s to 100s of cm deep) observed in the distal Gottero show similar geometrical relationships between deposit and substrate, comprising: i) sill-like sandstone extensions lateral to basal scours; ii) step-like lateral margins of scour features, and iii) flat and bed-parallel scoured surfaces. Therefore they can be interpreted as the result of the same kind of substrate interaction processes either frozen at different stages or variably expressed on account of different flow characteristics or position in relation to the zone of scouring. The absence anywhere along the bed base of a mud-draped erosion surface (mud-draped scours *sensu* Mutti and Normark, 1987) and the repeated association between scouring and the thicker mudstone clast-charged event beds suggest the scours were produced by the frontal part of the same gravity flow which deposited the overlying bed.

Mudstone clast and raft-bearing hybrid event beds

The beds overlying the scour features are interpreted to be hybrid event beds, namely complex beds made of a basal relatively clean sandstone deposited by turbiditic processes (hindered settling, basal near-bed high concentration layers and locally traction carpets) overlain by a muddy-sandstone with mudstone clasts and rafts interpreted as a debris flow or shearing low-strength bed layer (i.e. not

296 simply a mudstone clast-rich turbidite). The event beds are completed by a fine-grained graded and
297 laminated sandstone to mudstone couplet emplaced by the wake of the current which was again
298 more turbulent (Haughton et al., 2009; Fonnesu et al., 2015). As highlighted above, the size of the
299 entrained mudstone clasts centrally in the bed ranges widely from 5 to 25 cm across (Bed 14), to the
300 large mudstone rafts (2 meters up to 20 meters long) and pieces of folded thin-bed stratigraphy
301 contained in beds 5, 8, 15.4 and 17.3 (Fig. 5) which are surrounded by a mixture of sand and mud.

302 The presence in the examples discussed of abundant large mudstone clasts including very large rafts
303 resembling the immediate substrate preserved beneath less erosional parts of the event bed
304 suggests that in this case the entrainment happened following very local substrate erosion. As the
305 large substrate rafts are unlikely to have been carried in suspension, they are interpreted to have
306 collected near the bed following entrainment (Postma et al., 1988) and been driven for a relatively
307 short distance down flow within a shearing near-bed layer. Similar beds containing chaotic textures
308 at their base and interpreted to be related to the impact of dense turbidity currents upon a muddy
309 seafloor were described by Marschalko (1970) and Mutti and Normark, (1987). During transport, the
310 clasts were partly deformed and auto-injected by the matrix, in some cases spalling off smaller mud
311 flakes. The mud clast-rich part of the flow locally had sufficient energy to plough into the underlying
312 just deposited sand, accounting for the variable preservation of clean sandstone beneath it. These
313 beds were hence likely deposited by high-volume and catastrophic flows just after rapid substrate
314 entrainment without long-distance longitudinal flow transformation. The flows probably bypassed
315 the up-dip lobe region and just deposited on the confined basin plain (e.g. Mutti and Johns, 1978;
316 Remacha et al., 2005). The resulting hybrid event beds are texturally different (modest clay contents
317 and more abundant mudstone clasts) compared to the finer grained, usually mudstone clast-poor
318 (or with smaller mud chips) and better mixed sand-mud textures in hybrid event beds in unconfined
319 lobe systems elsewhere, such as parts of the Ross Formation (Pyles and Jennette, 2009), the Karoo
320 Fan in the Tanqua depocenter (Hodgson, 2009) or Paleogene Wilcox Fm. (Kane and Pontén, 2012).

Delamination features

Understanding the erosional/bypass phase of a flow is challenging as there is often limited associated deposition and the final erosional features that remain are composite and reveal little of how they initiated and grew (Stevenson et al., 2015). Different models have been proposed for the detachment of substrate beneath highly energetic turbulent flow phases by delamination ("hydraulic jacking" of Pickering and Corregiador, 2005; Puigdefàbregas et al., 2004; Eggenhuisen et al., 2011) or by shearing of scour edges within a mobile aggrading bed (Butler and Tavernelli, 2006; Clark and Stanbrook, 2001; Eggenhuisen et al., 2011). In the Gottero examples, the scour features have a complex asymmetric cross-sectional geometry (across flow) with wings of protruding sand extending into the substrate, forming detachment zones. Injections are generally coarse to very coarse-grained with a grain size similar to at the base of the event bed. These are interpreted as syn-depositional sand-injections. A post-depositional origin is considered unlikely as the top of the bed is never cross-cut by the injections (cf. Eggenhuisen et al., 2011). Moreover, the absence of deformation features in the underlying substrate or systematic rotation of mudstone clasts, exclude "shear in a mobile-aggrading substrate" (cf. Butler et al., 2016) as the active process in substrate delamination. Thus erosion by hydraulic jacking is the preferred model. The scour and associated injection features are very similar to those described by Eggenhuisen et al. (2010; 2011) from the Miocene Macigno Formation (NW Apennines, Italy) and the Champsaur Basin (SE France). Interestingly, the onset of the scouring and the incision of the grooves found in the Gottero case is the reverse of the relationship described by Eggenhuisen et al. (2010), with the grooves on Tier 1 in the Gottero Bed 14 pre-dating the scours that then excavated down to Tier 2. In the Champsaur and Macigno cases deeper scours were interpreted to cut first and then grooves ornamented the erosion surface.

The absence of bypass features such as abrupt grain-size breaks or large-scale cross-bedding (cf. Mutti, 1977; 1992; Stevenson et al., 2015) in any of the distal Gottero event beds suggests the multi-stage scours were produced during a single event (i.e. multiple scouring flows are unlikely to have

346 completely bypassed the area prior to sand deposition). The Gottero flows were strongly
347 depositional and even the substrate entrainment overlapped with just deposited sand injected
348 and/or drawn into bedding-parallel fractures beneath detaching clasts or rafts. The presence of
349 grooves and flutes at bed bases (as in the case of Tier 1, Bed 14 – Fig. 4A) implies initial passage of a
350 turbulent section of a current that was able to remove a superficial soft muddy layer and fashion
351 sole structures in the more indurated substrate beneath (Fig. 8). The initial shallow grooves can be
352 interpreted as produced by vortices in the flow head (Allen, 1982) and/or by the traction of mud
353 clasts and early diagenetic nodules (*septarie* nodules). Where the grooves were formed as tool
354 marks, they may have formed beneath an already more dense and stratified basal part of the flow in
355 which the clasts and nodules were embedded. During the following phase, deeper scours were
356 incised excavating the substrate and the just formed grooved surface. The lineated surface with a
357 fabric orthogonal to the paleoflow indicates internal uncoupling and flowage of the just deposited
358 sand close to the bed to the sites of injection. This suggests that following initial scour formation, the
359 substrate was not wholly excavated and removed by the by-passing head of the flow. Instead, the
360 head produced flow-parallel erosive steps that were then expanded by a process of lateral sand
361 injection and delamination. The substrate was already partly covered by just deposited sand or by a
362 dense sand-flow with liquefaction, when lateral pressure gradients drove intrusive sand into the
363 substrate exploiting mechanical heterogeneities in the underlying stratigraphy (see Puigdefàbregas
364 et al. 2004). Commonly, these injections were emplaced along the contact between stacked thin
365 beds and an underlying thick mudstone cap to an earlier event bed. The interface along which the
366 sand injections intruded then acted as a detachment plane. Additional sand may have been drawn
367 into detachment zones as the substrate rafts were rotated and released up into the flow where they
368 collected and were carried down flow *en-masse*. Groove casts on the Tier 2 surface indicate that the
369 flow was still sweeping the bed at this stage.

DISCUSSION

Scour initiation mechanisms

The presence of irregular seafloor topography was probably a prerequisite for injection-related delamination. Erosive steps would have focused lateral dynamic pressure venting of sand and water. Injection-related delamination features and related hybrid-like event beds have been observed onlapping or close to confining slopes in the Gres d'Annot by Puigdefàbregas et al. (2004). These authors describe sub-horizontal sand injections that delaminated earlier deposits forming chaotic bed divisions. In this case, delamination was related to the load and tangential stress of dense flows meeting a steep (c. 10°) counter slope. Although the distal Gottero Sandstone shows evidence of increasing confinement, an obvious confining slope is not preserved and there are no coherent spatial trends in terms of the abundance of delamination features with proximity to where the inferred confinement lay (to the NE). The layer-cake stratigraphy constrained by the bed-to-bed correlations in the M. Ramaceto section excludes the presence of significant pre-existing irregularities on the sea floor.

Irregularities in the substrate were therefore most likely produced by the flow itself in the form of the initial erosive scours which were then expanded by lateral injection and clast detachment. In some cases, the scour depth must have been of the order of the eventual bed itself, as in the case in example from M. Zatta (Fig. 6). The question then is how such erosion could be present in both outer fan lobes (M. Zatta) and confined basin plain (M. Ramaceto) settings with likely negligible axial gradients. Baas et al. (2009; 2011) and Sumner et al. (2009) suggested on the basis of experiments with clay-sand mixtures in open channels that a combination of high suspended-clay concentrations and rapid flow deceleration can produce a change from turbulent to transitional flow behavior. This model predicts that during the early stages of turbulence modification, the near-bed turbulence can actually increase before being damped as the flow decelerates. Transient turbulence enhancement might explain the presence of significant distal erosion. Thick mudstone caps on many of the larger

event beds imply the flows carried significant clay which is preserved on top of the beds due to the inferred ponded basin geometry. As the flows decelerated on low gradients having traversed the higher gradient fan system up dip, turbulence may have been enhanced under transitional flow conditions (Baas et al., 2009), triggering scouring and then delamination (Fig. 9A). Increasing stratification and turbulence modulation longitudinally along the flow might explain the tiering associated with progressively deeper downward excavation of scour surfaces prior to the onset of deposition.

An alternative or contributory explanation for the initial bed topography that seeded the injection and delamination process could relate to the structure of high-concentration and high-volume flows and the character of the substrate over which they advanced. Arrival of the flow front would induce a significant change in ambient pressure (Eggenhuisen and McCaffrey, 2012) that could deform a cohesive substrate before it was overrun by the body of the flow, causing fractures to open. Once the body arrived, higher fluid pressures would then force sand downwards into the fracture network which would expand laterally exploiting planes of weakness in the layered substrate, leading to delamination and the growth of large erosive patches (Fig. 9B). The presence of a strongly layered sheet system including extensive thick mudstone caps to beds may have promoted expansion by delamination. Part of the flow may even have dived below the seabed uplifting entire portions of compact stratigraphy (cf. *intrabed turbidites* of Baas et al., 2014 but here exploiting a fractured instead of a low-density fluid mud substrate). Substrate rafts and smaller mud clasts were then detached and segregated in the upper and rearward part of the flow where, if not buried by deposition, they may have been progressively destroyed by internal shearing (Fonnesu et al., 2015). The clay released could suppress flow turbulence down-dip (Baas et al., 2009; Haughton et al., 2009). Repeated pressure oscillations in the flow such as those present at the head-body transition (Best et al., 2005) and inside the body itself (e.g. large Kelvin-Helmholtz instabilities; Kneller and Buckee, 2000) could promote multistage injection and delamination accounting for the tiered structure. Across-flow lateral instability can be enhanced by counter-rotating streamwise vortices

(Hall et al., 2008) and this may have favored transverse expansion of initial defects at the expense of those that were at right angles to flow.

Whatever the mechanism triggering release of the clasts and rafts, it seems these were likely carried *en-masse* relatively short distances away from the site of erosion within an underflow in which the entrained substrate was broken up as it was injected by the sandy matrix which itself became progressively more contaminated by dispersed clay and clay chips. The dilute turbulent wake of the flow then deposited the upper fine-grained laminated sandstone which drapes the irregular top of the mudstone clast-rich central division (Haughton et al., 2009, Fonnesu et al., 2015).

Occurrence of hybrid event beds generated by substrate delamination

Mudstone clast-rich and raft bearing hybrid event beds are common in many deep-water systems in addition to the reported distal Gottero Sandstone examples (e.g. Marnoso Arenacea, Muzzi Magalhaes and Tinterri, 2010; Tinterri and Muzzi Magalhaes, 2011; Talling et al., 2012; Ventimiglia flysch, Marini et al., 2015b; Cilento Flysch, basal Ross Fm., Fonnesu et al., 2015; Castagnola Fm. Southern et al., 2015; Annot Sandstone; Patacci et al., 2014; Laga system; Mutti et al., 1978; Marini et al., 2015a). In some of them basal delamination features are reported (Puigdefàbregas et al., 2004, and see Fig. 5 of Southern et al., 2015) but in most cases these features have not been recognized, probably due to widespread and bed-parallel character of the entrainment meaning they are only revealed in cases where exceptional outcrop is preserved at km scale sufficient to allow detailed bed-by-bed correlation. Even in modern settings volumetrically important delamination in basin floor systems is likely to be overlooked because of immediate compensation by sediment deposited by the event responsible for the erosion. Nevertheless, many hybrid event beds in confined basin floor settings could form from large-volume and high-concentration flows by local delamination and mud entrainment. Thus the clasts may not have travelled very far and this could explain their local aspect, large size and the low degree of sand-mud mixing in the matrix surrounding them in comparison to other hybrid event bed types where values of mud content

446 percentage can vary between 25% and 80% (e.g. Sylvester and Lowe, 2004 and Talling et al., 2012). A
447 local mud source in the basin floor area (in contrast to an up-dip source envisaged in other settings
448 by Haughton et al., 2009) has the important consequence that the high degree of lateral
449 heterogeneity in terms of the variable proportion of the basal sandstone and upper muddy
450 sandstone within this type of hybrid event bed could be directly related to the original scour pattern
451 (Fonnesu et al., 2015). This means that the main parameters controlling the onset of hybrid flow in
452 this case are the mechanical properties of the substrate, in addition to the volume, velocity and
453 concentration of the flow. The stratigraphic pattern composed of a thick sandstone bed, overlain by
454 a thick mudstone cap and followed by a package of thin-bedded turbidites is common in the Gottero
455 outcrops (see Fig 2). These three components are likely to be deposited with different fabric and
456 water content and therefore to have different mechanical properties. The interface between a thick
457 mudstone cap and the thin-bedded sequence above appears to have behaved as a weak layer,
458 possibly due to the abrupt transition in mechanical properties from an homogenous medium to one
459 characterized by strong vertical heterogeneity. The presence of clasts and rafts clearly detached
460 from the substrate and incorporated into the overriding flow, and the propagation of fractures
461 infilled by sand to form injectites, suggests that the seafloor mud was cohesive and compact. This
462 type of firm but mechanically heterogeneous and multi-layered substrate including weak planes and
463 layers can be particularly prone to be delaminated. A stacking pattern of this type where intervals of
464 thin-bedded turbidites alternate with thick sandstone-mudstone couplets is characteristic of
465 confined basin plains developed in rapidly subsiding tectonically-active basins dominated by fine-
466 grained facies but occasionally filled by outsize sheet-like megabeds (Pilkey, 1987; Mutti and Johns,
467 1978; Remacha et al., 2005, Pickering and Hiscott, 2015). These settings can have rapid
468 sedimentation rates but an overall lower number of events in comparison to the more proximal fan
469 areas (Mutti and Johns, 1978; Mutti, 1992; Remacha et al., 2005), resulting in a lower frequency of
470 the events and a greater time available for the seafloor mud to dewater and be compacted.

Hodgson (2009) documented the common occurrence of mudstone clast-rich hybrid event beds at the top of interlobe sequences as the first events in overall thickening-upward more proximal lobe sequences in an unconfined setting (Karoo Basin). The occurrence of these HEBs could also be interpreted as related to the type of substrate (thick mudstone interlobe intervals) rather than to a change in gradient related to lobe avulsion. Conditions promoting distal delamination are likely to include large-volume early lowstand failures that trigger flows which carry sand across previous highstand mud drapes, and tectonically-triggered failures associated with particularly mobile flows that penetrate into otherwise fine-grained sectors of the basin floor.

Despite the presence of erosion in outer fan and confined basin plain areas, this is unlikely to contribute to increased sand-on-sand amalgamation and better vertical connectivity. Where documented so far, delamination develops within the intervening thick mudstones, expanding laterally rather than excavating vertically, therefore reducing the likelihood of sandstone layers becoming connected.

CONCLUSIONS

- Large scour features may be commonplace beneath mudstone clast-rich hybrid event beds in distal (confined basal plain and outer fan lobe) settings, but can be easily overlooked without exceptional laterally continuous exposures, and likely are similarly hard to detect in modern settings, due to associated sediment infill and compensation of erosional topography.
- Scours are inferred to start as small erosional features and develop through injection, hydraulic jacking and delamination processes during later stages of flow evolution under depositional and highly stratified conditions.
- Considerable erosion can occur with limited sediment bypass in sheet-like confined basin plains and outer fan lobes traversed by high-volume flows, in contrast with canyons,

channels and channel-lobe-transition environments where flows tend to bypass and erosional products are carried further down dip.

- Substrate delamination results in large mud clasts and substrate rafts that are incorporated into the flow and deposited as part of locally-generated hybrid event beds. It is inferred that clasts do not travel very far (they are sourced through delamination and do not become significantly disaggregated) and therefore the pattern of scours might control the heterogeneity within the intermediate muddy-sandstone division of the bed.
- Favorable conditions for substrate delamination are low-gradient and mud-rich cohesive substrates characteristic of outer fan lobe or confined basin plain settings, or other scenarios where large-volume flows traverse muddy and cohesive basin floors.

ACKNOWLEDGMENTS

This work was funded by Turbidites Research Group industry sponsors: Anadarko, BG-Group, BP, Conoco Phillips, Dana Petroleum, Maersk, Nexen, OMV, Petronas, Statoil, Tullow Oil and Woodside. We greatly thank Luca Baruffini for introducing us to the outcrops of M. Ramaceto area. Dave Hodgson, Ian Kane and an anonymous reviewer are gratefully acknowledged for their constructive comments which helped to improve an earlier version of the manuscript.

REFERENCES

Abbate, E., and Sagri, M., 1970. The eugeosynclinal sequences. Sedimentary Geology, 4(3), 251-340.

Allen, J. R. L., 1982. Sedimentary Structures: Their Character and Physical Basis. , 1256 pp.

Andri, E. and Zavatteri, F., 1990. Le septarie di Monte Mignano e de il Dente (Complesso di Monte Ramaceto, Appennino Ligure). Atti Soc. Tosc. Sc. Nat., Mem., 96, p. 1-48.

516 Baas, J.H., Best, J.L. and Peakall, J., 2011. Depositional processes, bedform development and hybrid
517 bed formation in rapidly decelerated cohesive (mud-sand) sediment flows. Sedimentology, 58, p.
518 1953-1987.

519 Baas, J.H., Best, J.L., Peakall, J. and Wang, M., 2009. A phase diagram for turbulent, transitional, and
520 laminar clay suspension flows. Journal of Sedimentary Research, 79, p. 162-183.

521 Baas, J. H., Manica, R., Puhl, E., Verhagen, I. and de O. Borges, A. L., 2014. Processes and products of
522 turbidity currents entering soft muddy substrates. Geology, 42, p. 371-374.

523 Beaubouef, R. T., Abreu, V. and Van Wagoner, J. C., 2003. Basin 4 of the Brazos-Trinity slope system,
524 western Gulf of Mexico: The terminal portion of a late Pleistocene lowstand systems tract. In:
525 Roberts, H. H., Rosen, N. C., Fillon, R. H. and Anderson, J. B. (Eds). GCSSEPM Foundation 23rd Annual
526 Research Conference, Shelf Margin Deltas and Linked Down Slope Petroleum Systems: Global
527 Significance and Future Exploration Potential, p. 45-66.

528 Best, J. L., Kostaschuk, R. A., Peakall, J., Villard, P. V. and Franklin, M., 2005. Whole flow field
529 dynamics and velocity pulsing within natural sediment-laden underflows. Geology, 33(10), p. 765-
530 768.

531 Bortolotti, V. and Passerini, P., 1970. Magmatic activity. Sedimentary Geology, 4(3), 599-624.

532 Brunt, R. L. and McCaffrey, W. D., 2007. Heterogeneity of fill within an incised channel: the
533 Oligocene Gres du Champsaur, SE France. Marine and Petroleum Geology, 24, p. 529-539.

534 Burgreen, B. and Graham, S., 2014. Evolution of a deep-water lobe system in the Neogene trench-
535 slope setting of the East Coast Basin, New Zealand: Lobe stratigraphy and architecture in a weakly
536 confined basin configuration. Marine And Petroleum Geology, 54, p. 1-22.

537 Butler, R. W. H. and Tavarnelli, E., 2006. The structure and kinematics of substrate entrainment into
538 high-concentration sandy turbidites: a field example from the Gorgoglione 'flysch' of southern Italy.
539 Sedimentology, 53(3), p. 655-670.

540 Butler, R. W., Eggenhuisen, J. T., Haughton, P., & McCaffrey, W. D., 2016. Interpreting
541 syndepositional sediment remobilization and deformation beneath submarine gravity flows; a
542 kinematic boundary layer approach. Journal of the Geological Society, 173(1), p. 46-58.

543 Casnedi, R., 1982. Sedimentazione e tettonica della unità liguri nell'Appennino nord-occidentale
544 (Valli Lavagna-Sturla Trebbia e Aveto). Atti Ist. Geol. Univ. Pavia, 30, p. 42-66.

545 Clark, J. D. and Stanbrook, D. A., 2001. Formation of large-scale shear structures during deposition
546 from high-density turbidity currents, Gres d'Annot Formation, south-east France. In: McCaffrey, W.
547 D., Kneller, B. C. and Peakall, J. (Eds). Particulate Gravity Currents. Special Publication of the
548 International Association of Sedimentologists, Oxford, Blackwell, 31, p. 219-232.

549 Eggenhuisen, J. T. and McCaffrey, W. D., 2012. The vertical turbulence structure of experimental
550 turbidity currents encountering basal obstructions: implications for vertical suspended sediment
551 distribution in non-equilibrium currents. Sedimentology 59(3), p. 1101-1120.

552 Eggenhuisen, J. T., McCaffrey, W. D., Haughton, P. D. W. and Butler, R. W. H., 2010. Small-Scale
553 Spatial Variability in Turbidity-Current Flow Controlled by Roughness Resulting from Substrate
554 Erosion: Field Evidence for a Feedback Mechanism. Journal of Sedimentary Research 80(1-2), p. 129-
555 136.

556 Eggenhuisen, J. T., McCaffrey, W. D., Haughton, P. D. W. and Butler, R. W. H., 2011. Shallow erosion
557 beneath turbidity currents and its impact on the architectural development of turbidite sheet
558 systems. Sedimentology 58(4), p. 936-959.

559 Elter, P., and Raggi, G., 1965. Contributo alla conoscenza dell'Appennino ligure, 3. Tentativo di
560 interpretazione delle brecce ofiolitiche cretacee in relazione con movimenti orogenetici
561 nell'Appennino ligure. Boll. Soc. Geol. Ital, 84(5), p. 1-12.

562 Etienne, S., Mulder, T., Bez, M., Desaubliaux, G., Kwasniewski, A., Parize, O., Dujoncquoy, E. and
563 Salles, T., 2012. Multiple scale characterization of sand-rich distal lobe deposit variability: Examples
564 from the Annot Sandstones Formation, Eocene-Oligocene, SE France. Sedimentary Geology, 273, p.
565 1-18.

566 Fildani, A., Hubbard, S. M., Covault, J. A., Maier, K. L., Romans, B. W., Traer, M. and Rowland, J. C.,
567 2013. Erosion at inception of deep-sea channels. Marine And Petroleum Geology, 41, p. 48-61.

568 Fonnesu, F., 2003. 3D seismic images of a low-sinuosity slope channel and related depositional lobe
569 (West Africa deep-offshore). Marine and Petroleum Geology, 20(6-8), p. 615-629.

570 Fonnesu, M., Haughton, P. D. W., Felletti, F. and McCaffrey, W. D., 2015. Short length-scale
571 variability of hybrid event beds and its applied significance. Marine and Petroleum Geology, 67, p.
572 583-603.

573 Hall, B., Meiburg, E. and Kneller, B. C., 2008. Channel formation by turbidity currents: Navier-Stokes-
574 based linear stability analysis. Journal of Fluid Mechanics, 615, p. 185-210.

575 Haughton, P. D. W., 2001. Contained turbidites used to track sea bed deformation and basin
576 migration, Sorbas Basin, south-east Spain. Basin Research, 13(2), p. 117-139.

577 Haughton, P.D.W., Barker, S.P. and McCaffrey, W.D., 2003. “Linked” debrites in sand-rich turbidite
578 systems – origin and significance. Sedimentology, 50, p. 459-482.

579 Haughton, P.D.W., Davis, C.E. and McCaffrey, W.D., 2009. Hybrid sediment gravity flow deposits –
580 Classification, origin and significance. Marine and Petroleum Geology, 26, p. 1900-1918.

581 Hodgson, D. M., 2009. Distribution and origin of hybrid beds in sand-rich submarine fans of the
582 Tanqua depocentre, Karoo Basin, South Africa. Marine and Petroleum Geology, 26, p. 1940-1956.

583 Hodgson, D. M., Flint, S. S., Hodgetts, D., Drinkwater, N. J., Johannessen, E. P. and Luthi, S. M., 2006.
584 Stratigraphic evolution of fine-grained submarine fan systems, Tanqua depocenter, Karoo Basin,
585 South Africa. Journal of Sedimentary Research, 76(1-2), p. 20-40.

586 Hofstra, M., Hodgson, D. M., Peakall, J. and Flint, S. S., 2015. Giant scour-fills in ancient channel-lobe
587 transition zones: Formative processes and depositional architecture. Sedimentary Geology, 329, p.
588 98-114.

589 Hubbard, S. M., Covault, J. A., Fildani, A. and Romans, B. W., 2014. Sediment transfer and deposition
590 in slope channels: Deciphering the record of enigmatic deep-sea processes from outcrop. Geological
591 Society of America Bulletin, 126(5-6), p. 857-871.

592 Johnson, S. D., Flint, S. S., Hinds, D. and Wickens, H. d. V., 2001. Anatomy, geometry and sequence
593 stratigraphy of basin floor to slope turbidite systems, Tanqua Karoo, South Africa. Sedimentology,
594 48(5), p. 987-1023.

595 Kane, I.A. and Pontén, A.S.M., 2012. Submarine transitional flow deposits in the Paleogene Gulf of
596 Mexico. Geology, 40, n. 12, p. 1119-1122.

597 Kneller, B. C. and Buckee, C., 2000. The structure and fluid mechanics of turbidity currents: a review
598 of some recent studies and their geological implications. Sedimentology, 47(1), p. 62-94.

599 Kneller, B.C., and McCaffrey, W.D., 2003. The interpretation of vertical sequences in turbidite beds:
600 the influence of longitudinal flow structure. Journal of Sedimentary Research, 73, p. 706-713.

601 Kolla, V., 2007. A review of sinuous channel avulsion patterns in some major deep-sea fans and
602 factors controlling them. Marine and Petroleum Geology 24, p. 450-469.

603 Marini, M., 1992. L'unita del M. Gottero fra la Val Trebbia e Sestri Levante (Appennino Ligure); nuovi
604 dati di analisi di bacino e ipotesi di evoluzione sedimentaria. Boll. Soc. Geol. It., 111(1), p. 3-23.

605 Marini, M., 1995. Le arenarie del Monte Gottero nell'areale del Monte Zatta (Unita del Monte
606 Gottero, Appennino Ligure). Boll. Soc. Geol. It., 114(3), p. 575-598.

607 Marini, M., Milli, S., Ravnås, R. and Moscatelli, M., 2015a. A comparative study of confined vs. semi-
608 confined turbidite lobes from the Lower Messinian Laga Basin (Central Apennines, Italy):
609 Implications for assessment of reservoir architecture. Marine and Petroleum Geology, 63, p. 142-
610 165.

611 Marini, M., Patacci, M., Felletti, F., Cerliani, A., Azzarone, M., Decarlis, A., McCaffrey W.D., 2015b.
612 The depositional architecture of Mass Transport Deposits from the Ventimiglia Flysch Fm. (Eocene,
613 NW Italy): implications for seafloor reshaping and turbidite deposition. IAS meeting Krakov 22-25
614 June 2015.

615 Marroni, M., 1991. Deformation history of the M.Gottero Unit (Internal Ligurid Units, Northern
616 Apennines). Boll. Soc. Geol. It., 110, p. 727-736.

617 Marroni, M., and Pandolfi, L., 2001. Debris flow and slide deposits at the top of the Internal Liguride
618 ophiolitic sequence, Northern Apennines, Italy: A record of frontal tectonic erosion in a fossil
619 accretionary wedge. Island Arc, 10(1), p. 9-21.

620 Marroni, M., Meneghini, F. and Pandolfi, L, 2004. From accretion to exhumation in a fossil
621 accrectionary wedge: a case history from Gottero unit (Northern Apennines, Italy). Geodinamica
622 Acta, 17, p. 41-53.

623 Marschalko, R., 1970. The origin of disturbed structures in Carpathian turbidites. Sedimentary
624 Geology, 4, p.5-18.

Mayall, M. and Stewart, I., 2000. The architecture of turbidite slope channels. In: GCSSEPM Foundation 20th Annual Research Conference, Deep-Water Reservoirs of the World, p. 578-586.

Monechi, S. and Treves B., 1984. Osservazioni sull'età delle Arenarie del Gottero: Dati del nannoplancton calcareo. Ofioliti, 9(1), p. 93-96, ISSN: 0391-2612.

Mutti, E. and Johns, D. R., 1978. The role of sedimentary by-passing in the genesis of fan fringe and basin plain turbidites in the Hecho Group system (South-central Pyrenees). Memorie della Società Geologica Italiana, Rome, Italy, Società Geologica Italiana, 18, p. 15-22.

Mutti, E. and Normark, W. R., 1987. Comparing examples of modern and ancient turbidite systems; problems and concepts. In: Leggett, J. K. and Zuffa, G. G. (Eds). Marine clastic sedimentology; concepts and case studies. London, United Kingdom, Graham and Trotman, p. 1-38.

Mutti, E., 1977. Distinctive thin-bedded turbidite facies and related depositional environments in the Eocene Hecho Group (South-central Pyrenees, Spain). Sedimentology, 24(1), p. 107-131.

Mutti, E., 1992. Turbidite sandstones. San Donato Milanese, Agip, 275 pp.

Mutti, E., Bernoulli, D., Ricci Lucchi, F. and Tinterri, R., 2009. Turbidites and turbidity currents from Alpine 'flysch' to the exploration of continental margins. Sedimentology, 56(1), p. 267-318.

Mutti, E., Nilsen, T. H. and Ricci Lucchi, F., 1978. Outer fan depositional lobes of the Laga Formation (upper Miocene and lower Pliocene), East-Central Italy. In: Stanley, D. J. and Kelling, G. (Eds). Sedimentation in submarine canyons, fans, and trenches. Stroudsburg, Pa., United States, Dowden, Hutchinson & Ross, Inc., p. 210-222.

Mutti, E., Sonnino, 1981. Compensational cycles: A diagnostic feature of turbidite sandstone lobes. In: Abstract volume of International Association of Sedimentologists, Second European Regional Meeting, Bologna, Italy, p. 120-123.

647 Muzzi Magalhaes, P. and Tinterri, R., 2010. Stratigraphy and depositional setting of slurry and
648 contained (reflected) beds in the Marnoso-arenacea Formation (Langhian-Serravallian) Northern
649 Apennines, Italy. Sedimentology, 57(7), p. 1685-1720.

650 Nilsen, T.H. and Abbate, E., 1984. Submarine-Fan facies associations of the Upper Cretaceous and
651 Paleocene Gottero Sandstone, Ligurian Apennines, Italy. Geo-Marine Letters, 3, p. 193-197.

652 Pandolfi, L., 1997. Stratigrafia ed evoluzione strutturale delle succession torbiditiche cretacee della
653 Liguria orientale (Appennino Settentrionale). PhD thesis, Università di Pisa, 175 pp.

654 Parea, G.C., 1965. La provenienza dei clastici dell'arenaria del M.Gottero. Atti e Mem. Acc. Naz. Sci.
655 Lett. e Arti. Modena, ser 6, 6, 7 pp.

656 Passerini, P., and Pirini, C., 1964. Microfaune paleoceniche nelle formazioni dell'Arenaria del
657 M.Ramaceto e degli argilloscisti di Cichero. Boll. Soc. Geol. Ital., 83(6), p. 15-28.

658 Patacci, M., 2016. A high-precision Jacob's staff with improved spatial accuracy and laser sighting
659 capability. Sedimentary Geology, 335, p. 66-69.

660 Patacci, M., Haughton, P. D. W. and McCaffrey, W. D., 2014. Rheological complexity in sediment
661 gravity flows forced to decelerate against a confining slope, Braux, SE France. Journal of Sedimentary
662 Research, 84(4), p. 270-277.

663 Patacci, M., Haughton, P. D. W. and McCaffrey, W. D., 2015. Flow Behavior of Ponded Turbidity
664 Currents. Journal of Sedimentary Research, 85(8), p. 885-902.

665 Pickering, K. T. and Corregidor, J., 2005. Mass-transport complexes, (MTCs) and tectonic control on
666 basin-floor submarine fans, middle eocene, south Spanish Pyrenees. Journal of Sedimentary
667 Research, 75(5), p. 761-783.

668 Pickering, K. T. and Hiscott, R. N., 1985. Contained (reflected) turbidity currents from the Middle
669 Ordovician Cloridorme Formation, Quebec, Canada; an alternative to the antidune hypothesis.
670 Sedimentology, 32(3), p. 373-394.

671 Pickering, K. T. and Hiscott, R. N., 2015. Deep Marine Systems: Processes, Deposits, Environments,
672 Tectonics and Sedimentation. American Geophysical Union, Wiley, 672 pp.

673 Pilkey, O. H., 1987. Sedimentology of basin plains. In: Weaver, P. P. E. and Thomson, J. (Eds). Geology
674 and geochemistry of abyssal plains. Geological Society of London Special Publication, London, UK,
675 Geological Society of London, 31, p. 1-12.

676 Piper, D. J. W. and Normark, W. R., 2001. Sandy fans: from Amazon to Hueneme and beyond. AAPG
677 Bulletin, 85(8), p. 1407-1438.

678 Pirmez, C., Beaubouef, R. T., Friedmann, S. J. and Mohrig, D. C., 2000. Equilibrium Profile and
679 Baselevel in Submarine Channels: Examples from Late Pleistocene Systems and Implications for the
680 Architecture of Deepwater Reservoirs. In: GCSSEPM Foundation 20th Annual Research Conference,
681 Deep-Water Reservoirs of the World, p. 782-805.

682 Postma, G., Nemec, W. and Kleinspehn, K. L., 1988. Large floating clasts in turbidites; a mechanism
683 for their emplacement. Sedimentary Geology, 58(1), p. 47-61.

684 Prélat, A. and Hodgson, D. M., 2013. The full range of turbidite bed thickness patterns in submarine
685 lobes: controls and implications. Journal of the Geological Society of London, 170(1), p. 209-214.

686 Prélat, A., Hodgson, D. M. and Flint, S. S., 2009. Evolution, architecture and hierarchy of distributary
687 deep-water deposits: a high-resolution outcrop investigation from the Permian Karoo Basin, South
688 Africa. Sedimentology, 56(7), p. 2132-2154.

689 Puigdefàbregas, C., Gjelberg, J. and Vaksdal, M., 2004. The Gres d'Annot in the Annot syncline: outer
690 basin-margin onlap and associated soft-sediment deformation. In: Joseph, P. and Lomas, S. A. (Eds).

691 Deep-Water Sedimentation in the Alpine Basin of SE France: New Perspectives on the Gres D'Annot
692 and Related Systems. Geological Society of London Special Publication, 221, p. 367-388.

693 Pyles, D.R. and Jennette, D.C., 2009. Geometry and architectural associations of co-genetic debrite-
694 turbidite beds in basin-margin strata, Carboniferous Ross Formation (Ireland): Applications to
695 reservoirs located on the margins of structurally confined submarine fans. Marine and Petroleum
696 Geology, 26, p. 1974-1996.

697 Remacha, E., Fernandez, L.P, and Maestro, E., 2005. The transition between sheet-like lobe and
698 basin-plain turbidites in the Hecho Basin (South-Central Pyrenees, Spain). Journal of Sedimentary
699 Research, 75, 798-819.

700 Sinclair, H. D. and Tomasso, M., 2002. Depositional evolution of confined turbidite basins. Journal of
701 Sedimentary Research, 72(4), p. 451-456.

702 Southern, S. J., Patacci, M., Felletti, F. and McCaffrey, W. D., 2015. Influence of flow containment
703 and substrate entrainment upon sandy hybrid event beds containing a co-genetic mud-clast-rich
704 division. Sedimentary Geology, 321, p. 105-122.

705 Stevenson, C.J., Jackson, C.A.L., Hodgson, D.M., Hubbard, S.M. and Eggenhuisen, J.T., 2015. Deep-
706 Water sediment bypass. Journal of Sedimentary Research, 85, p. 1058-1081.

707 Sumner, E. J., Talling, P. J. and Amy, L. A., 2009. Deposits of flows transitional between turbidity
708 current and debris flow. Geology, 37(11), p. 991-994.

709 Sylvester, Z. and Lowe, D. R., 2004. Textural trends in turbidites and slurry beds from the Oligocene
710 flysch of the East Carpathians, Romania. Sedimentology, 51(5), p. 945-972.

711 Talling, P. J., 2013. Hybrid submarine flows comprising turbidity current and cohesive debris flow:
712 Deposits, theoretical and experimental analyses, and generalized models. Geosphere, 9(3), p. 460-
713 488.

714 Talling, P. J., Amy, L. A., Wynn, R. B., Peakall, J. and Robinson, M., 2004. Beds comprising debrite
715 sandwiched within co-genetic turbidite: origin and widespread occurrence in distal depositional
716 environments. Sedimentology, 51(1), p. 163-194.

717 Talling, P. J., Malgesini, G., Sumner, E. J., Amy, L. A., Felletti, F., Blackbourn, G., Nutt, C., Wilcox, C.,
718 Harding, I. C. and Akbari, S., 2012. Planform geometry, stacking pattern, and extrabasinal origin of
719 low strength and intermediate strength cohesive debris flow deposits in the Marnoso-arenacea
720 Formation, Italy. Geosphere, 8(6), p. 1207-1230.

721 Tinterri, R. and Muzzi Magalhaes, P., 2011. Synsedimentary structural control on foredeep turbidites:
722 An example from Miocene Marnoso-arenacea Formation, Northern Apennines, Italy. Marine and
723 Petroleum Geology, 28(3), p. 629-657.

724 Van der Merwe, W. C., Hodgson, D. M., Brunt, R. L. and Flint, S. S., 2014. Depositional architecture of
725 sand-attached and sand-detached channel-lobe transition zones on an exhumed stepped slope
726 mapped over a 2500 km^2 area. Geosphere, 10(6), p. 1076-1093.

727 Wynn, R. B., Kenyon, N. H., Masson, D. G., Stow, D. A. V. and Weaver, P. P. E., 2002. Characterization
728 and recognition of deep-water channel-lobe transition zones. AAPG Bulletin, 86(8), p. 1441-1462.

729 ## FIGURE CAPTIONS

730 **Figure 1**. Geological map of the Gottero turbidite system and summary stratigraphy. A) Simplified
731 geological and location map of the Gottero system with approximate distribution of main facies
732 associations and the paleocurrent pattern (modified from Nilsen and Abbate, 1984); the rectangle
733 outlines the area considered in this study. The black line indicated as “Bracco High” represents the
734 inferred location of an intra-basinal high and potential external basin boundary (Elter and Raggi,
735 1965). B) Internal Liguridi basin stratigraphy (modified from Marroni, 1991) with an expanded
736 section for the Gottero succession in the M. Ramaceto section. The main interpreted sub-
737 environments and the stratigraphic position of the beds referred to in the text are indicated.

738 **Figure 2.** Architecture of the upper Gottero stratigraphy in the M. Ramaceto section. A) Correlation
739 panel of the M. Ramaceto succession between beds 11 and 16 (between 188 and 285 m below the
740 top of the formation), highlighting the tabular geometry and correlativity of individual beds at km-
741 scale albeit with local erosion into the substrate. Datum plane is the base of a mudstone interval rich
742 in carbonate nodules ("Septarie level"). B) Panoramic photo of the northern side of the M. Ramaceto
743 succession, showing measured log locations, the main faults (red lines) and the base of the Giaiette
744 chaotic unit (Giaiette MTC). The stratigraphic interval between the two white dashed lines
745 corresponds to the interval shown in the overlying correlation panel; trace of Bed 14 (see Figs. 3 and
746 4) is highlighted in yellow. Note the succession is overturned. C) Close-up of the highlighted interval
747 in Fig. 2B showing the sheet-like geometry of the succession in which individual beds can be traced
748 (note bed amalgamation is very rare).

749 **Figure 3.** Depositional and erosional features of Bed 14 at M. Ramaceto (Outcrop location – Latitude:
750 44°25'10.80"N; Longitude: 9°18'15.35"E). A) Bed 14 facies stack and outcrop photograph (note the
751 succession is upside-down due to tectonic folding) at Log C, and relative grain to dispersed clay
752 (G/M) abundance calculated from thin-section point counting. B) Lateral variability of the mudstone
753 clast-rich intermediate division of Bed 14 on a 10s to 100s of meters scale. Scours are observed at
754 most locations. However, the planform geometry can only be characterized where the inverted bed
755 base forms an extensive dip-slope (3C). Numbers refer to levels of substrate erosion observed (T1,
756 T2, T3). C) Basal scours planform and close-up of the main outcrop areas showing geometries of the
757 scour margins.

758 **Figure 4** Basal surface of Bed 14. A) Schematic illustration of the terraced geometry of the scour
759 surface, the underlying limestone bed is used as a datum; B) Rose diagrams representing the
760 direction of the overall paleoflow indicators collected on the base of Bed 14 base and subdivided by
761 tier; C) cross-cutting relationship between Tier 1 grooves and Tier 2 scours on the southern side of
762 the outcrop; D) three levels of substrate erosion captured in the northern side of the outcrop; E)

step-like and wing-like edges of scour features that tend to coalesce and form a compound erosional surface (2 m laser Jacob's staff for scale); F) Undercut margin associated with mud clast detachment; G) Lineation fabric oriented perpendicular to the paleoflow in sandstone just above Tier 2 broken scours. Circled numbers in all parts of the figure refers to the tier level of the surface.

Figure 5. Event bed correlations in M. Ramaceto area showing differential substrate delamination using correlated beds beneath as datum planes; the examples are conservative estimates of the amount of erosion as it cannot be determined whether the erosion surfaces continue to cut up and down section outside of the correlation panel.

Figure 6. Delamination process of substrate rafts at the base of an hybrid event bed in M. Zatta area. A) Detail correlation of a bed sequence in M. Zatta area capturing delamination of 1.1 meters of thin-bedded stratigraphy (log 8). B) Outcrop view in log 8 location capturing a 20 m length substrate slab containing thin-bedded interval (a) and lateral extension of an underlying sand injection (b). C) Close-up of the source of the sand injection and lateral deformation of the substrate in the act of being detached. D) Detail from log 3, showing texture of mudstone clast-rich dirty sandstone (c) and shape of substrate clast containing thin-bedded stratigraphy (d) torn from the underlying seafloor and buried in the bed (40 cm ruler for scale).

Figure 7. Raft-bearing hybrid event beds and relationship with their substrate. A) Raft-bearing bed from M. Zatta succession with a 3 m long muddy raft (highlighted by dashed line) containing scattered limestone nodules, encapsulated in a mudstone clast-rich dirty sandstone and capped by fine-grained and laminated clean sandstone (arrowed). B) Bed from M. Zatta succession including a deformed thin-bedded raft resembling the underlying substrate. C) Bed 5 from M. Ramaceto succession in log E (see Fig. 5) containing a 8 m long substrate raft in which there are thin beds. (*b*: base of the bed; *t*: top of the bed).

Figure 8. Phases of flow evolution and interactions with substrate in a strike-view.T1) Flow mostly bypassing and incising shallow sole structures (grooves and flutes) on sea floor; T2) Incision of elongated scours; T3) Intrusion of basal sand layer into underlying substrate exploiting weak interfaces in the thin-bedded package and expanding laterally in a direction perpendicular to paleoflow, with associated uplift of substrate rafts and mud clasts; T4) Bed aggradation and deposition of muddy rafts and mud clasts collected via a similar mechanism immediately upstream, which are in the process of disaggregation following internal shearing and upward sand injections from the overpressured basal sand. Red curves represent idealized flow concentration profiles.

Figure 9. Alternative initiation mechanisms for substrate delamination in a section along the depositional dip. A) Substrate scouring due to enhanced turbulence (see Baas et al., 2009; 2011) followed by dense flow substrate delamination; B) Substrate weakening and deformation by oscillating pressure followed by dense flow substrate delamination. Note most of the delamination occurs in the across flow direction where wing-like scour margins are preferentially preserved (see Fig. 8). HDF: high-density flow; LDF: low-density flow.

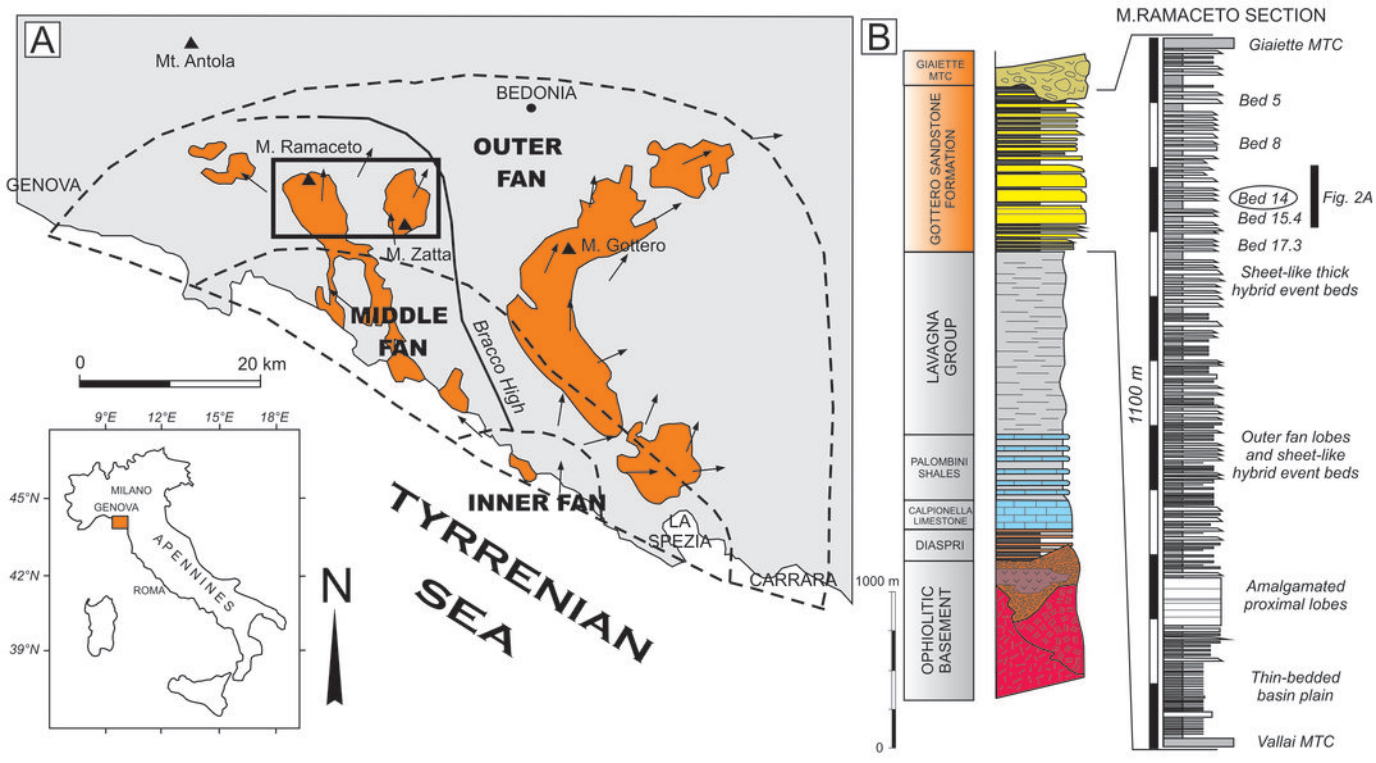
A
Mt. Antola
BEDONIA
M. Ramaceto
GENOVA
OUTER FAN
M. Zatta
M. Gottero
MIDDLE FAN
Bracco High
0
20 km
9°E
12°E
15°E
18°E
45°N
42°N
39°N
MILANO
GENOVA
APENNINES
ROMA
N
INNER FAN
TYRRENIAN SEA
LA SPEZIA
CARRARA
B
M.RAMACETO SECTION
GIAIETTE MTC
GOTTERO SANDSTONE FORMATION
LAVAGNA GROUP
PALOMBINI SHALES
CALPIONELLA LIMESTONE
DIASPRI
OPHIOLITIC BASEMENT
1000 m
0
1100 m
Giaiette MTC
Bed 5
Bed 8
Bed 14
Bed 15.4
Fig. 2A
Bed 17.3
Sheet-like thick hybrid event beds
Outer fan lobes and sheet-like hybrid event beds
Amalgamated proximal lobes
Thin-bedded basin plain
Vallai MTC

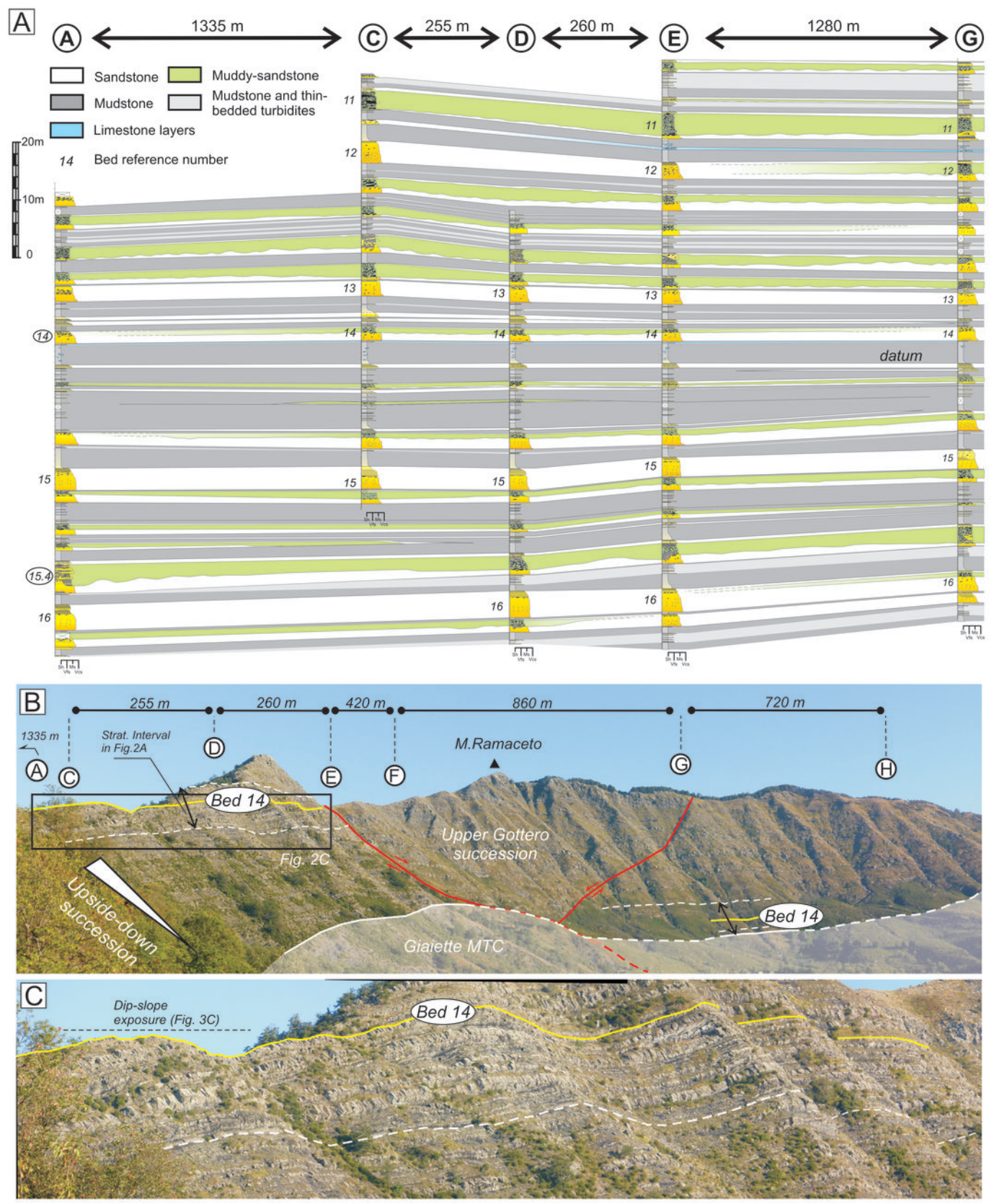
A
1335 m
255 m
260 m
1280 m
Sandstone
Muddy-sandstone
Mudstone
Mudstone and thin-bedded turbidites
Limestone layers
14 Bed reference number
20m
10m
0
datum
B
255 m
260 m
420 m
860 m
720 m
1335 m
Strat. Interval in Fig.2A
M.Ramaceto
Bed 14
Fig. 2C
Upper Gottero succession
Upside-down succession
Gialette MTC
C
Dip-slope exposure (Fig. 3C)
Bed 14

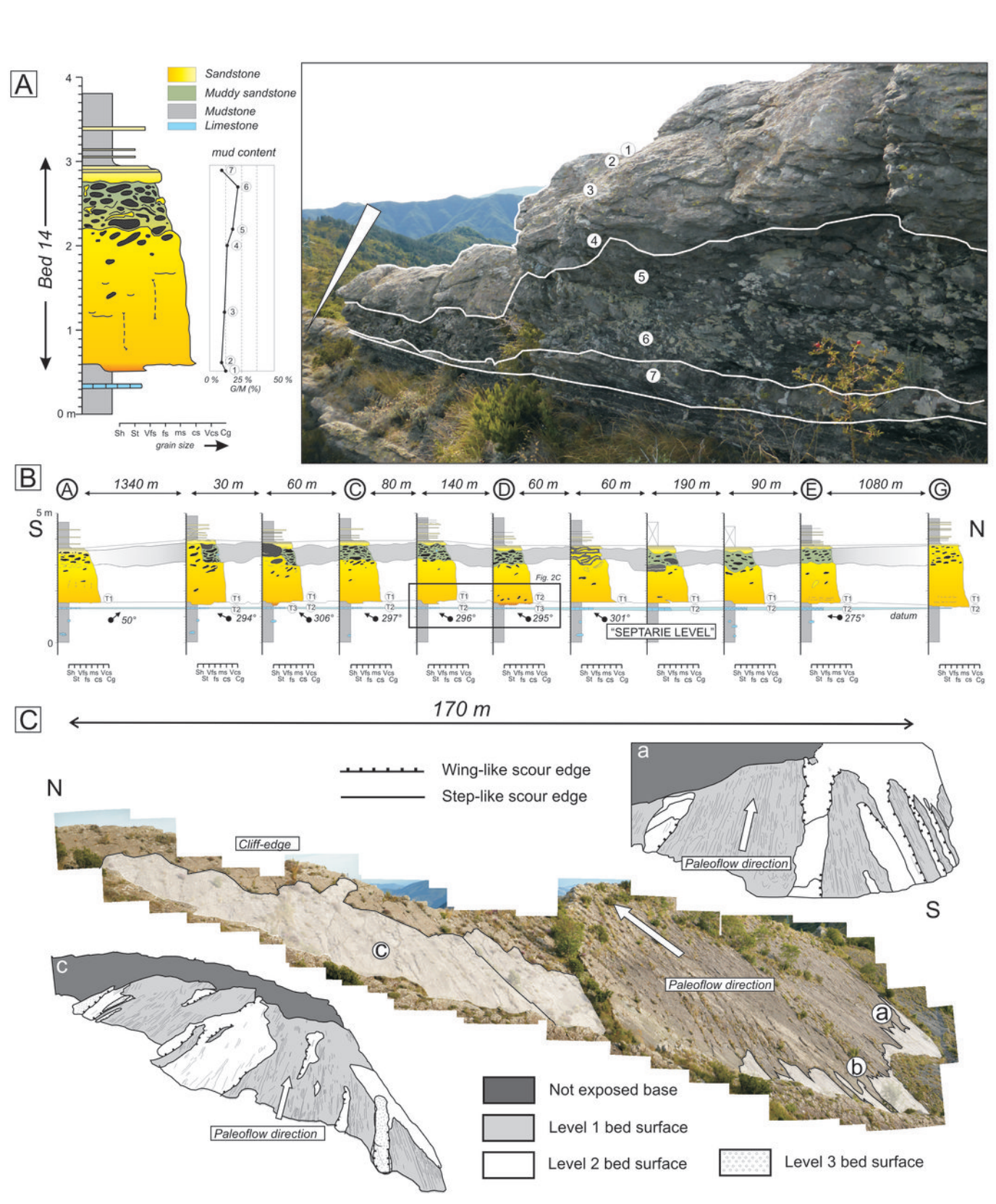
A
Sandstone
Muddy sandstone
Mudstone
Limestone
mud content
Bed 14
0 m
grain size
Sh St Vfs fs ms cs Vcs Cg
0 %
25 %
50 %
G/M (%)
B
1340 m
30 m
60 m
80 m
140 m
60 m
60 m
190 m
90 m
1080 m
S
N
5 m
0
Fig. 2C
50°
294°
306°
297°
296°
295°
301°
"SEPTARIE LEVEL"
275°
datum
C
170 m
N
S
Wing-like scour edge
Step-like scour edge
Cliff-edge
Paleoflow direction
Paleoflow direction
Paleoflow direction
Not exposed base
Level 1 bed surface
Level 2 bed surface
Level 3 bed surface

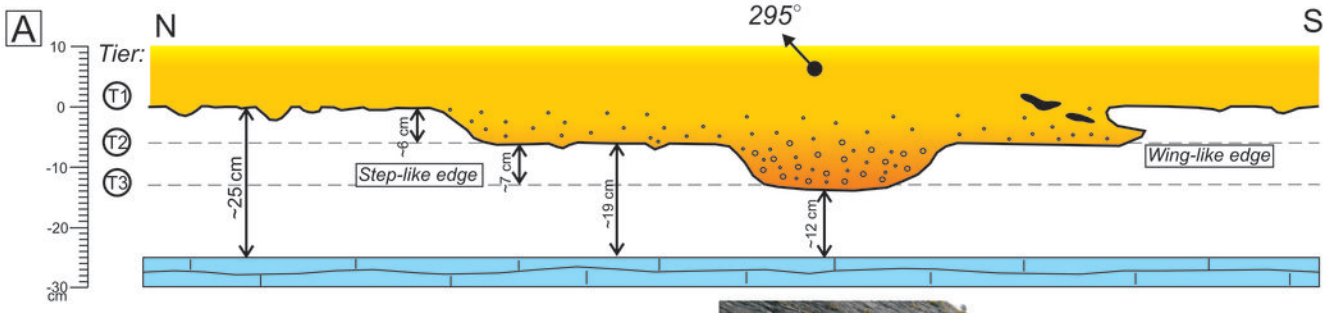
A
N
295°
S
Tier:
T1
T2
T3
10
0
-10
-20
-30
cm
~6 cm
~25 cm
Step-like edge
~7 cm
~19 cm
~12 cm
Wing-like edge

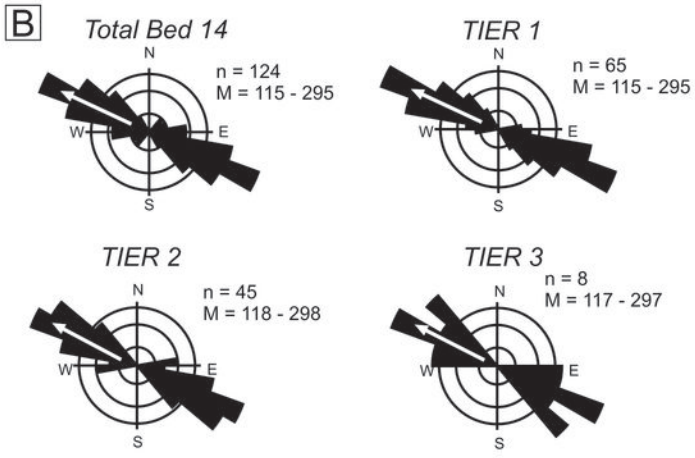
B
Total Bed 14
n = 124
M = 115 - 295
TIER 1
n = 65
M = 115 - 295
TIER 2
n = 45
M = 118 - 298
TIER 3
n = 8
M = 117 - 297
N
E
S
W

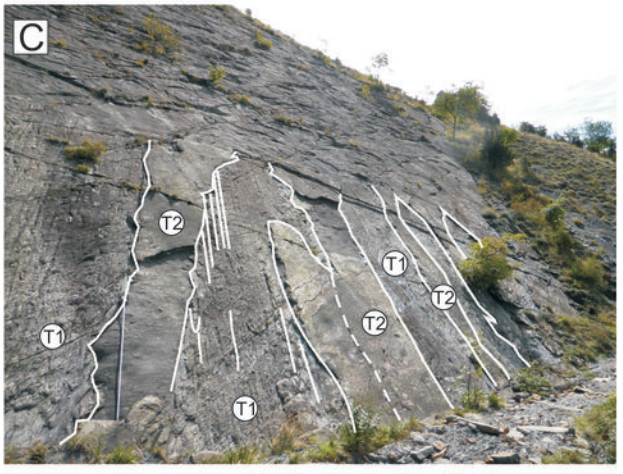
C
T1
T2

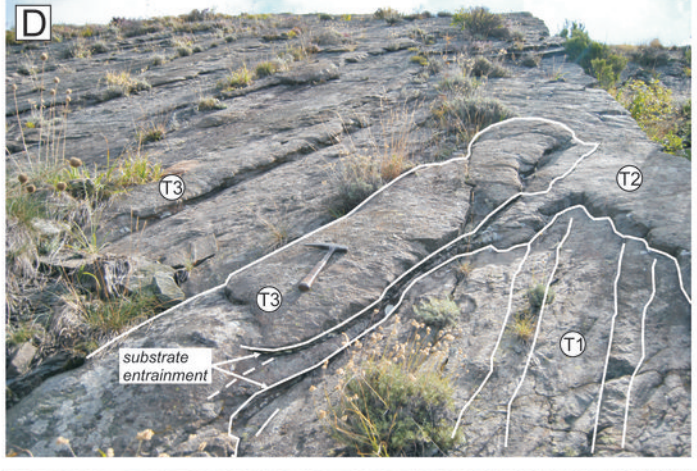
D
T1
T2
T3
substrate entrainment

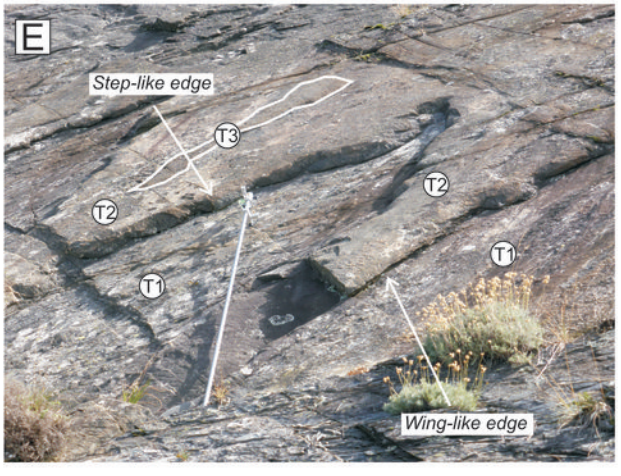
E
Step-like edge
T1
T2
T3
Wing-like edge

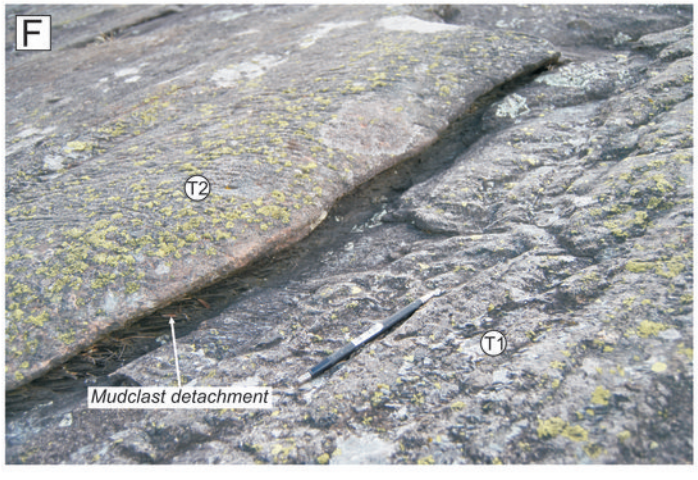
F
T1
T2
Mudclast detachment

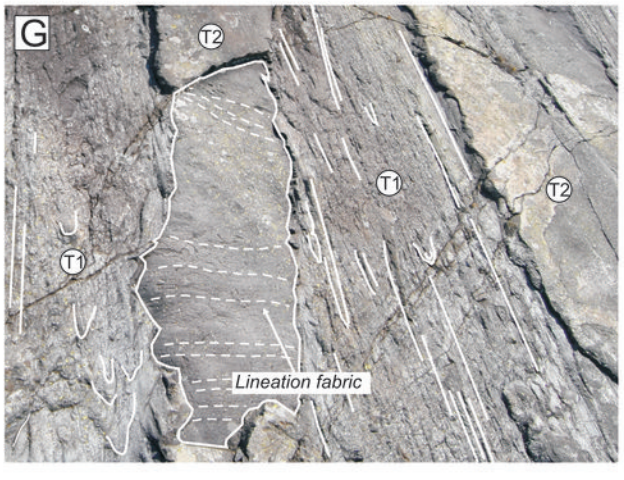
G
T1
T2
Lineation fabric

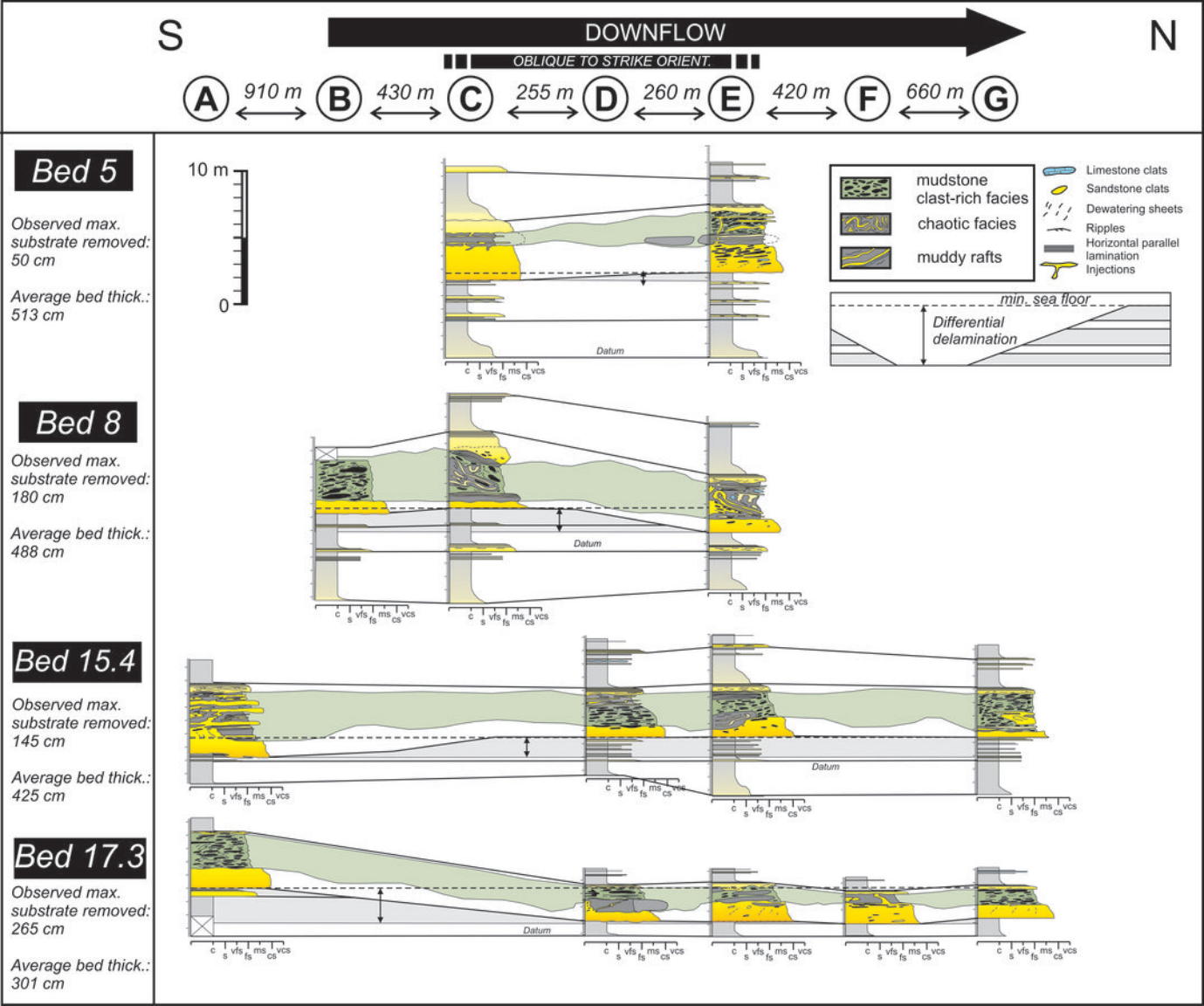
S
DOWNFLOW
N
OBLIQUE TO STRIKE ORIENT.
A
910 m
B
430 m
C
255 m
D
260 m
E
420 m
F
660 m
G
Bed 5
Observed max. substrate removed: 50 cm
Average bed thick.: 513 cm
Bed 8
Observed max. substrate removed: 180 cm
Average bed thick.: 488 cm
Bed 15.4
Observed max. substrate removed: 145 cm
Average bed thick.: 425 cm
Bed 17.3
Observed max. substrate removed: 265 cm
Average bed thick.: 301 cm
10 m
0
Datum
c s vfs fs ms cs vcs
mudstone clast-rich facies
chaotic facies
muddy rafts
Limestone clats
Sandstone clats
Dewatering sheets
Ripples
Horizontal parallel lamination
Injections
min. sea floor
Differential delamination

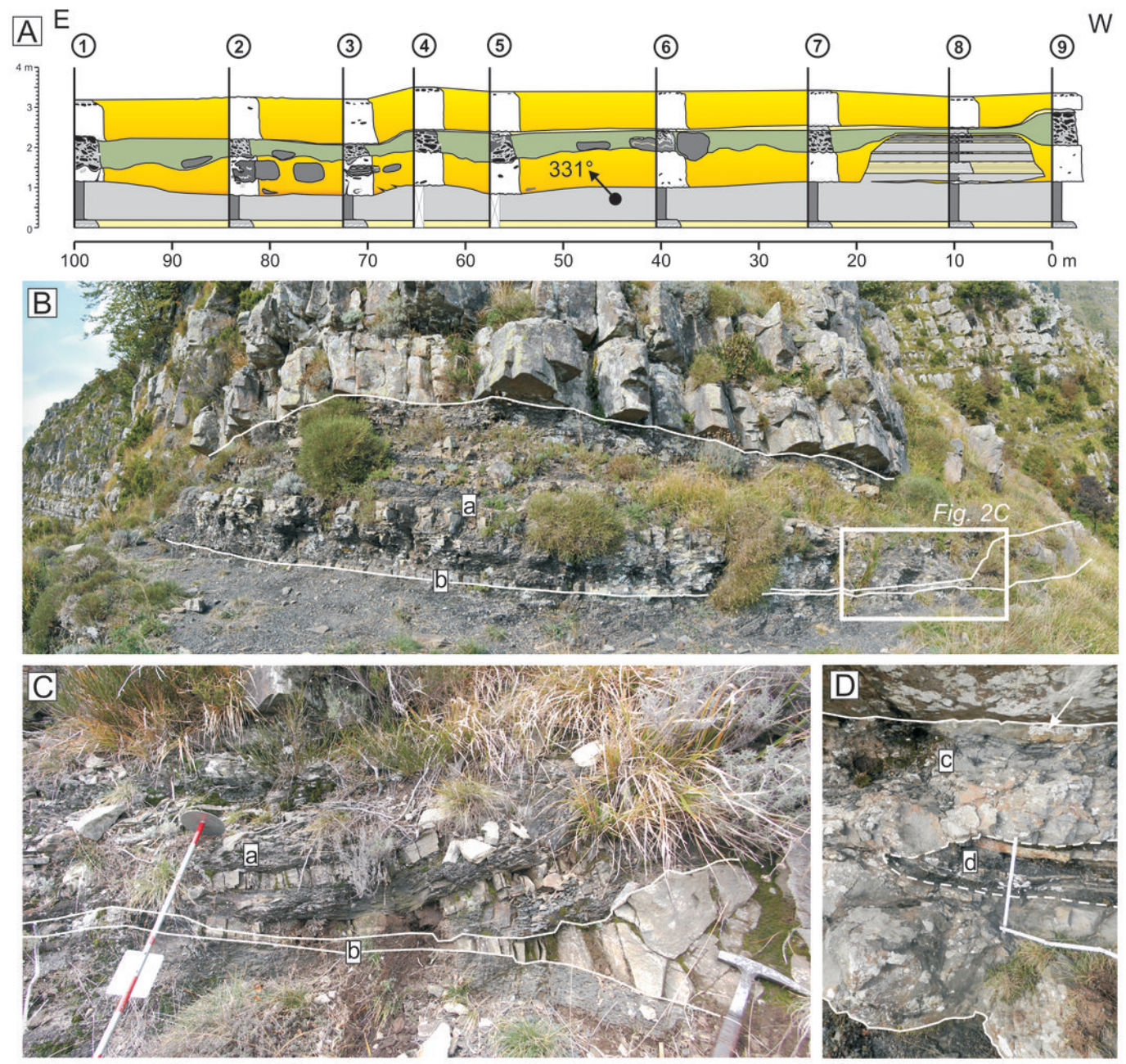
A
E
W
1
2
3
4
5
6
7
8
9
4 m
3
2
1
0
331°
100
90
80
70
60
50
40
30
20
10
0 m
B
a
b
Fig. 2C
C
a
b
D
c
d

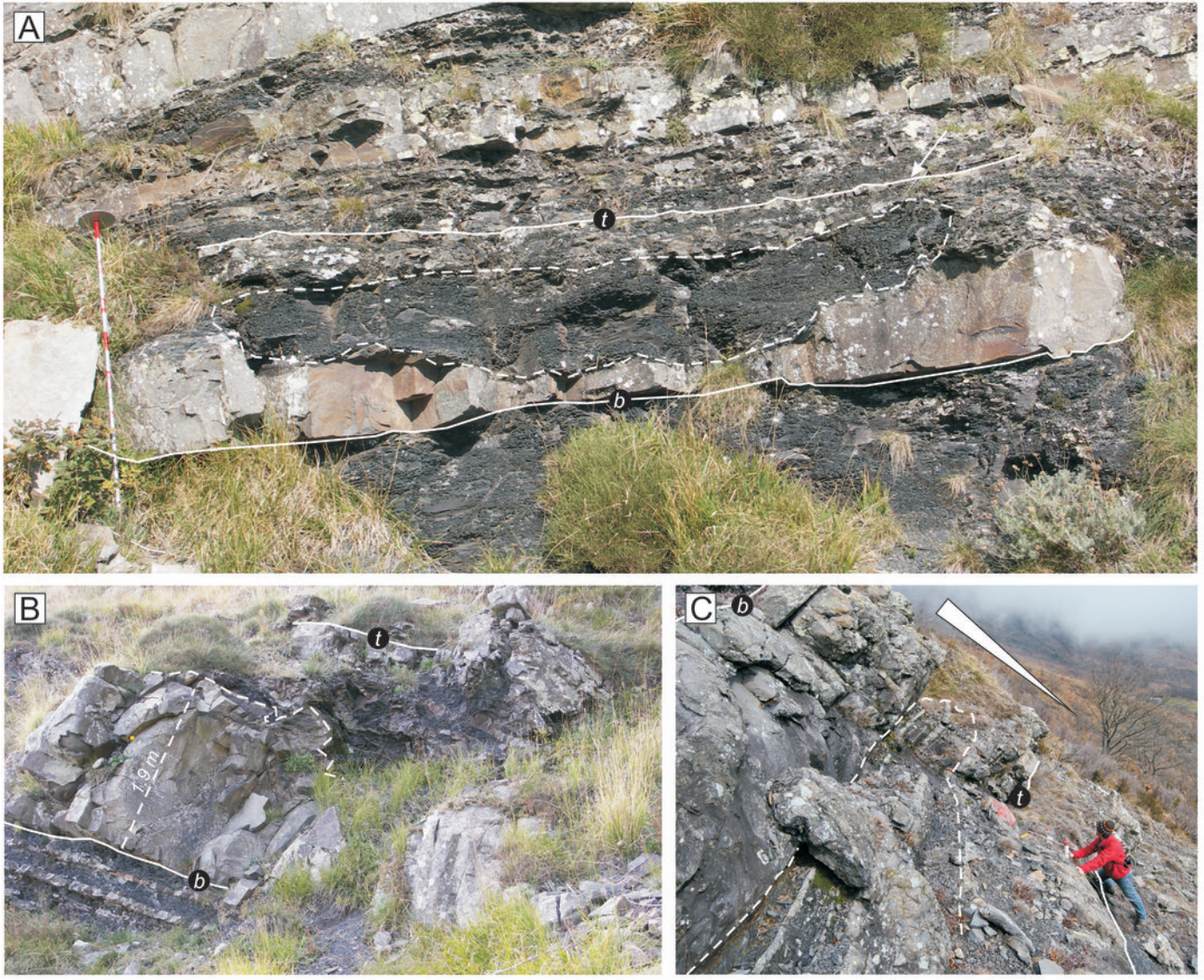
A
t
b
B
t
1.9 m
b
C
b
t

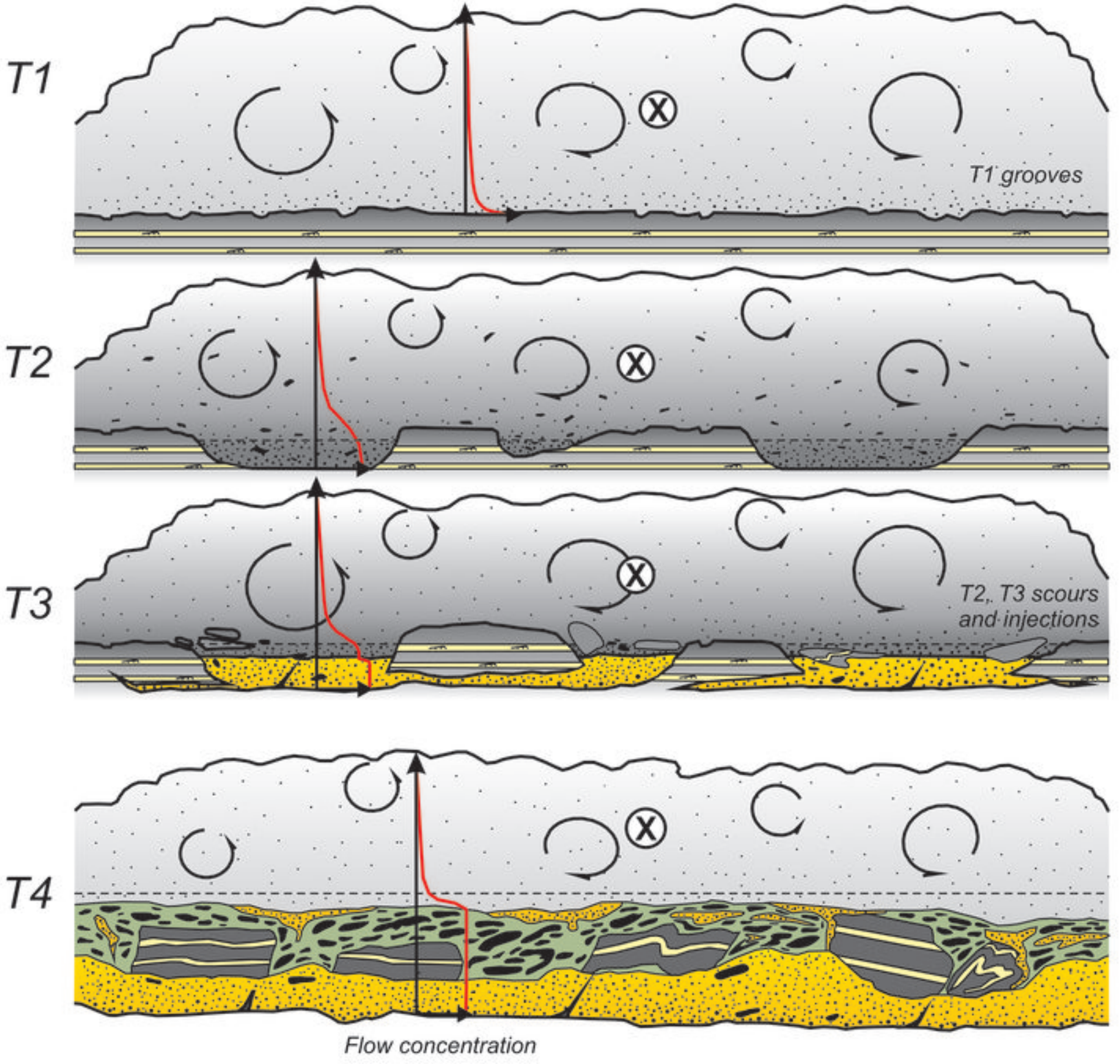
T1
T1 grooves
T2
T3
T2, T3 scours
and injections
T4
Flow concentration

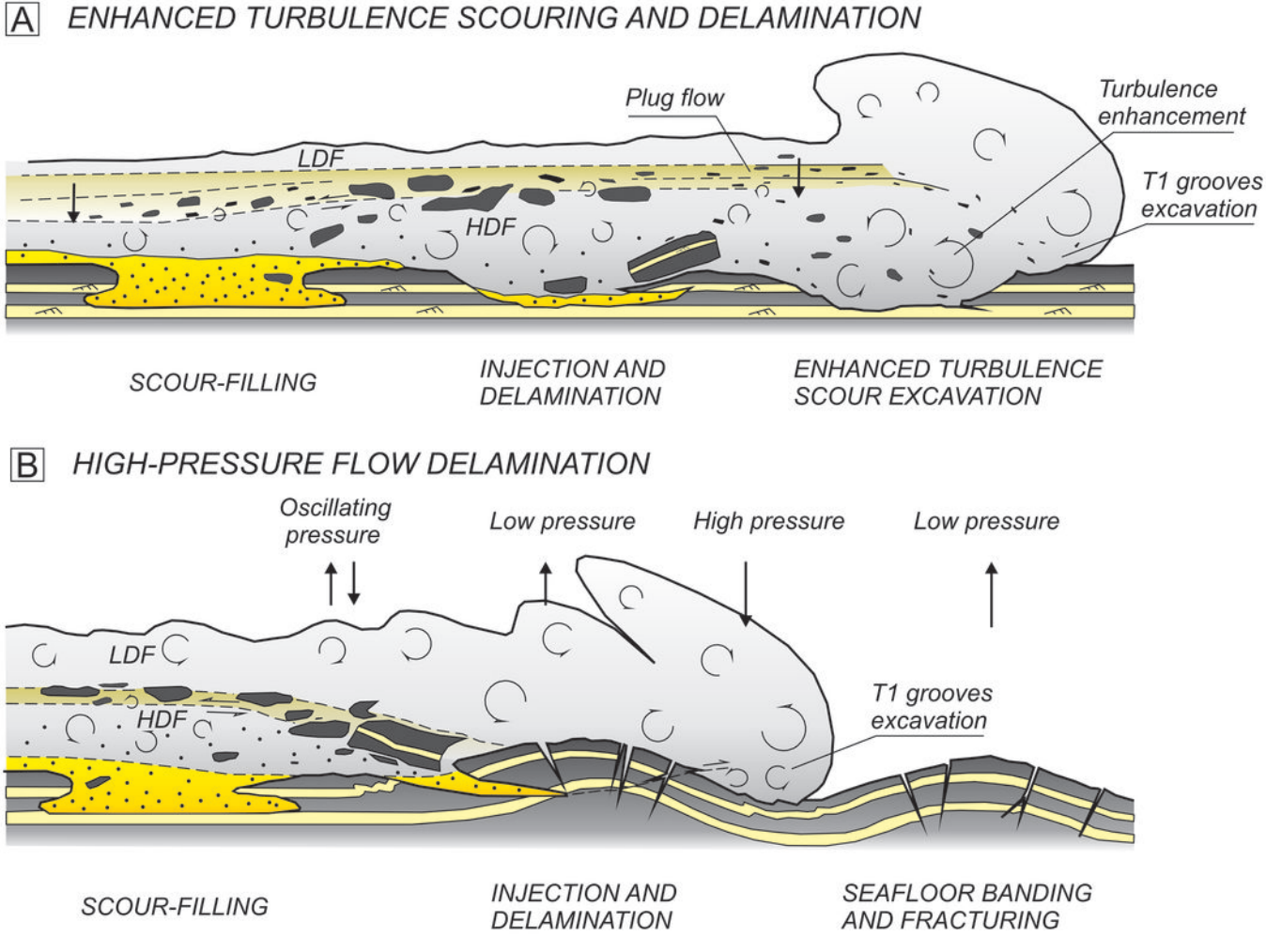
A
ENHANCED TURBULENCE SCOURING AND DELAMINATION
Plug flow
Turbulence enhancement
LDF
HDF
T1 grooves excavation
SCOUR-FILLING
INJECTION AND DELAMINATION
ENHANCED TURBULENCE SCOUR EXCAVATION
B
HIGH-PRESSURE FLOW DELAMINATION
Oscillating pressure
Low pressure
High pressure
Low pressure
LDF
HDF
T1 grooves excavation
SCOUR-FILLING
INJECTION AND DELAMINATION
SEAFLOOR BANDING AND FRACTURING